NJC

Dynamic Article Links

Cite this: *New J. Chem.*, 2012, **36**, 1596–1609

www.rsc.org/njc

PAPER

Hydrophobic-exterior layer structures and magnetic properties of trinuclear copper complexes with chiral amino alcoholate ligands†

Jana K. Maclaren,[a] Joaquín Sanchiz,*[b] Pedro Gili[b] and Christoph Janiak*[a]

Received (in Victoria, Australia) 28th January 2012, Accepted 21st April 2012
DOI: 10.1039/c2nj40063d

The trinuclear secondary building unit (SBU) $\{Cu_3(\mu\text{-}L)_4X_2\}$ constructed from chelating and alcoholate-*O*-bridging chiral amino alcoholate (amino alkoxido, μ-L) and terminal halide ligands (X) gives rise to two-dimensional (2D) homochiral supramolecular polymers through the bridging action of the halide ligand. Compounds 2D-$[Cu_3(\mu\text{-}L)_4(\mu_3\text{-}X)_2]$ {X = Br (**1** to **4**), X = Cl (**5**, **6**); L = amino-ethanolate (**1**, **5**), (*R*)-2-amino-propan-1-olate (**2**), (*R*)-2-amino-butan-1-olate (ab) (**3**, **6**), (*R*)-2-amino-2-phenyl-ethanolate (**4**)} were synthesized from 2-amino alcohol, LH with $CuBr_2$ or $CuCl_2$, respectively, in the presence of triethylamine (TEA). The crystal packing of isomorphous 2D-$[Cu_3(\mu\text{-}L)_4(\mu_3\text{-}X)_2]$ shows a separation of the hydrophobic alkyl from the hydrophilic amino-/alcoholate-/Cu–Br-region. Charge-assisted $Cu^{(2+)}\cdots^{(-)}Br$- and hydrogen-bonding interactions in the hydrophilic region are the driving force of "hydrophobic exterior layer" formation with a hydrophilic interior exposing the hydrophobic alkyl groups to the exterior. Stacking of the layers through weak van-der-Waals interactions between the alkyl groups correlates with formation of thin crystal plates along the stacking direction. A lower ligand concentration yields both dinuclear and mononuclear SBUs in one-dimensional (1D-) homochiral coordination polymers 1D-$[\{Cu_2(\mu\text{-ab})_2Br_2\}_2\{(\mu_3\text{-Br})Cu(abH)_2Br\}\{(\mu_3\text{-Br})Cu(abH)(CH_3OH)Br\}]$ (**7**) and 1D-$[\{Cu_2(\mu\text{-ab})_2Cl_2\}_2\{(\mu_3\text{-Cl})Cu(abH)(CH_3CH_2OH)Cl\}_2]$ (**8**). In $\{[Cu(rac\text{-abH})(rac\text{-ab})H_2O]ClO_4\}_2$ (**9**) two SBUs combine through charge assisted H-bonds to a dimeric unit. Temperature dependent magnetic susceptibility measurements of **1** and **3** show ferromagnetic coupling but no magnetic ordering. However, at temperatures lower than 3 K an onset of long-range magnetic ordering can be observed. AC magnetic measurements in the range of 1.9 K to 5 K at different frequencies show that the long range magnetic ordering is achieved at lower temperatures than that. Correlation of magnetic coupling with the Cu–O–Cu angle is in agreement with the structural parameters of **1** and **3**. Very good agreement between experimental and DFT calculated *J*,*j* coupling constants shows that the interaction between the terminal copper(II) ions in these linear trinuclear SBUs is operative and it cannot be neglected.

Introduction

There is ongoing work in the formation of chiral coordination polymers,[1–4] *e.g.*, for chiral catalysis[5,6] or enantiomer recognition.[7] Two main strategies exist: (i) homochiral ligands as linkers to connect the metal atoms or clusters; (ii) homochiral chelating or terminal ligands to assemble homochiral secondary building units (SBUs)[8] which then can be connected *via* achiral linkers or a combination of both.[6,9]

Both types of homochiral ligands should preferably come from the chiral pool.

Homochiral bridging ligands include saccharate,[10] aspartate,[11] lactate,[12] tartarate,[13] citramalate,[14] malate,[15,16] mandelate,[16] camphorate[17] and bridging ligands constructed from amino acids.[18] Enantiopure chelating ligands are aminocarboxylates (amino acetates/acids),[19,20] (*R*/*S*)-1,1′-bi-2-naphthol/-ate (BINOL)[21] and derivatives, (*R*/*S*)-(aryl)ethylamines for chiral Schiff bases,[22] and others[23] for the formation of SBUs for extended (one- to three-dimensional) structures. The search for suitable SBUs is one aspect of the crystal engineering of hybrid inorganic–organic framework materials. Amino alcohol ligands have been shown to lead to very versatile SBUs.[24–30]

Ongoing work on metal complexes with easily accessible amino alcoholate (amino alkoxido) ligands[24–30] prompted us

[a] *Institut für Anorganische Chemie und Strukturchemie, Universität Düsseldorf, Universitätsstr. 1, D-40225 Düsseldorf, Germany. E-mail: janiak@uni-duesseldorf.de*
[b] *Grupo de Materiales Magnéticos, Departamento de Química Inorgánica, Universidad de La Laguna, La Laguna 38206, Spain. E-mail: jsanchiz@ull.es*

† Electronic Supplementary Information (ESI) available: X-ray powder diffractograms, IR spectra, H-bonding details, packing diagrams, photographs of experimental setups. CCDC reference numbers 864924–864928. For ESI and crystallographic data in CIF or other electronic format see DOI: 10.1039/c2nj40063d

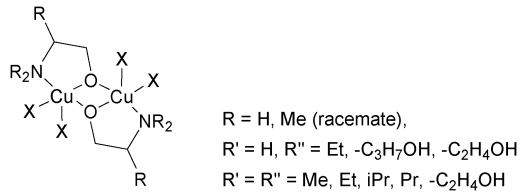

Scheme 1 Common binuclear copper building unit with amino alcoholate (amino alkoxide) derivatives in coordination polymers; X = coordination sites occupied by bridging ligands (see text).

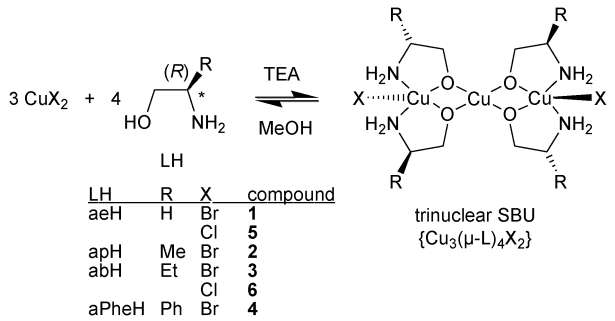

LH	R	X	compound
aeH	H	Br	**1**
		Cl	**5**
apH	Me	Br	**2**
abH	Et	Br	**3**
		Cl	**6**
aPheH	Ph	Br	**4**

Scheme 2 Bulk synthesis of compounds **1** to **6** with their trinuclear SBU.

to utilize *chiral* amino alcoholate ligands for the formation of homochiral SBUs for extended coordination polymeric structures. Known structures with the enantiopure β-amino alcoholate ligands[31] 2-amino-propan-1-olate (ap),[32–34] 2-amino-butan-1-olate (ab),[34,35] (*S*)-2-amino-2-phenylethanolate (aPhe),[20,36] 2-amino-3-methyl-pentan-1-olate,[33] (1*S*,2*S*)-(+)-1-phenyl-2-amino-1,3-dihydroxypropanolate,[37] D(−)-1,2-diphenyl-2-oxyethylamine,[38] (*S*)-phenylalaninolate,[39] 2-amino-1-phenyl-propan-1-olate (norphedrine),[33,40] are so far restricted to molecular metal complexes.[20,31–40]

Coordination polymers with alcoholato-*O*-bridged binuclear copper ethanolamine complexes as SBUs have been reported (Scheme 1). These SBUs are connected with bridging ligands (X), such as 1,2-bis(4-pyridyl)ethylene,[26] pyrazine,[27] p-bis(4-pyridyl)-benzene, 9,10-bis(4-pyridyl)anthracene, bis-(4-pyridyl)disulfide, tris(3-pyridyl)benzene,[25] 3-hydroxobenzoate,[28] acetate[29] or with pseudo halogenides.[30] However, the amino alcoholate ligands used were either achiral or racemic mixtures.

Here we report homochiral 2D- and 1D-coordination polymers built up from the chiral novel trinuclear SBU $\{Cu_3(\mu\text{-}L)_4X_2\}$,[5] the dinuclear SBU $\{Cu_2(\mu\text{-}L)_2X_2\}$ and the mononuclear SBUs $\{Cu(LH)_2Br_2\}$ and $\{Cu(LH)(solvent)X_2\}$, respectively, with X = Cl, Br and the chiral amino alcohols (LH) (*R*)-2-amino-propan-1-ol (*R*-apH), (*R*)-2-amino-butan-1-ol (*R*-abH), (*R*)-2-amino-2-phenyl-ethanolate (*R*-aPheH) and achiral 2-amino-ethanol (aeH) for comparison (*cf.* Scheme 2).

Results and discussion

2D coordination polymers with trinuclear copper SBUs

Bulk materials of compounds **1–6** were obtained quantitatively by treating the amino alcohol with triethylamine, TEA and anhydrous CuX_2 (X = Br for compounds **1** to **4** and Cl for **5** and **6**) in the ratio 4 : 4 : 3 (slight excess of amino alcohol) in methanol (Scheme 2). All compounds were analyzed by powder X-ray diffraction, IR and elemental analysis.

Crystals of sufficient quality for single-crystal X-ray diffraction by slow reactant diffusion of the amino alcohol and copper salt could only be obtained for **1** and **3**. Representative nature and identity to the bulk sample was established by comparison of the X-ray powder pattern calculated from the single crystal data with a measured diffractogram of the bulk material. Many failed attempts were made to crystallize the (*R*)-amino alcoholate complexes **2**, **4–6**. Compared to the crystallization from achiral amino ethanolate we can note difficulties when trying to crystallize from enantiopure ligands,[41] which is consistent with difficulties that we experienced when trying to crystallize (*R*)- or (*S*)-1,1′-bi-2-naphtholate metal salts[21,42] or (*R*)-1,1′-binaphthalene-2,2′-diyl phosphate salts.[43]

Similarity of the X-ray powder diffractograms for compounds **1–6** (Fig. S1–S5 in ESI†) suggests that all six compounds have a similar structure as elucidated for **1** and **3** by single-crystal investigation. Due to the orientation of the residues the layer distances are different (*cf.* Table 2) and therefore the structures are not entirely isostructural, which leads to shifts within the powder diffractograms. However from the combination of the X-ray powder diffractograms and the MIR and FIR spectra (Fig. S6–S9 in ESI†) we can conclude that structures **1–6** within one layer are built up from the same SBUs connected through the halogenide anions in the same way as in the structures **1** and **3** for which a single crystal structure solution exists. This is also in agreement with the analogy of compounds **1** and **3**. The neutral copper SBU consists of three Cu(II) cations, two halide and four deprotonated amino alcoholate ligands (Fig. 1, *cf.* Scheme 2). The three Cu(II) cations are linearly arranged and connected through the oxo-atoms from the deprotonated amino alcohol. The amino alcoholate

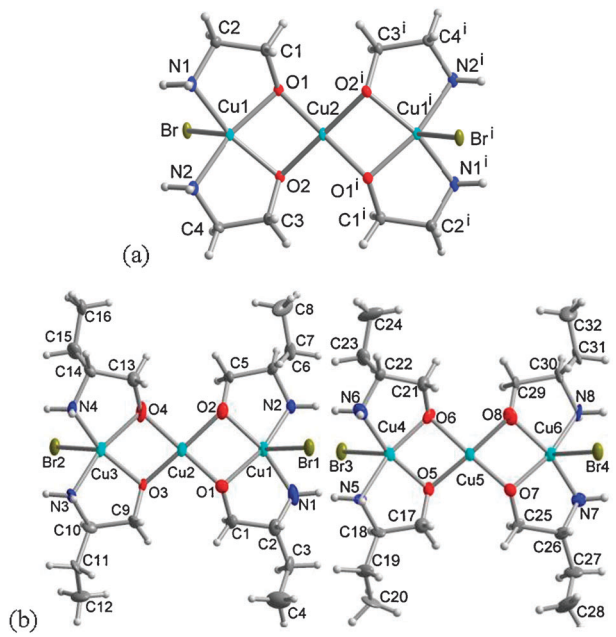

Fig. 1 SBUs of compounds **1** (a) and **3** (b) (two symmetry-independent units) (50% thermal ellipsoids for non-hydrogen atoms); symmetry operation: (i) = 1 − *x*, 1 − *y*, −*z*; distances and angles in Table 1.

Table 1 Selected bond lengths (Å) and angles (°) in **1** and **3**[a]

Compound **1**			
Cu1–O1	1.971(3)	O1–Cu1–O2	81.48(12)
Cu1–O2	1.965(3)	O1–Cu1–N1	86.99(13)
Cu1–N1	1.993(4)	O1–Cu1–N2	164.30(13)
Cu1–N2	1.991(4)	O2–Cu1–N1	163.90(13)
Cu1–Br	2.7799(7)	O2–Cu1–N2	87.10(14)
Cu2–O1	1.981(3)	N1–Cu1–N2	101.85(16)
Cu2–O2	1.973(3)	Br–Cu1–Br$^{(iii)}$	172.18(3)
		O1–Cu1–Br	103.10(8)
Cu1···Cu2	2.8163(5)	N1–Cu1–Br	90.01(10)
		Cu1–O1–Cu2	90.92(12)
Cu1···Br$^{(iii)}$	3.1614(8)	Cu1–O2–Cu2	91.29(12)
Cu2···Br$^{(iii)}$	3.0072(5)	O1–Cu2–O2	81.04(12)
		O1–Cu2–O2$^{(i)}$	98.96(12)
		O1–Cu2–Br$^{(iii)}$	86.54(8)

Compound **3**							
First SBU				Second SBU			
Cu1–O1	1.983(16)	O1–Cu1–O2	82.2(6)	Cu4–O5	1.924(16)	O5–Cu4–O6	82.6(6)
Cu1–O2	1.951(17)	O1–Cu1–N1	86.4(7)	Cu4–O6	1.952(19)	O5–Cu4–N5	86.3(6)
Cu1–N1	1.99(3)	O1–Cu1–N2	160.8(7)	Cu4–N5	1.994(19	O5–Cu4–N6	162.6(8)
Cu1–N2	1.965(18)	O2–Cu1–N1	163.3(8)	Cu4–N6	2.01(2)	O6–Cu4–N5	164.5(7)
Cu1–Br1	2.764(4)	O2–Cu1–N2	85.7(6)	Cu4–Br3	2.775(4)	O6–Cu4–N6	86.7(7)
		N1–Cu1–N2	101.8(7)			N5–Cu4–N6	101.3(7)
Cu2–O1	1.961(15)	O1–Cu1–Br1	104.6(5)	Cu5–O5	1.964(15)	O5–Cu4–Br3	103.7(5)
Cu2–O2	1.999(16)	Cu2–Cu1–Br1	127.91(13)	Cu5–O6	1.998(16)	N5–Cu4–Br3	127.84(13)
Cu2–O3	1.940(15)	Cu1–O1–Cu2	91.4(6)	Cu5–O7	1.984(15)	Cu4–O5–Cu5	92.7(6)
Cu2–O4	1.977(17)	Cu1–O2–Cu2	91.2(7)	Cu5–O8	1.992(17)	Cu4–O6–Cu5	90.8(7)
		O1–Cu2–O2	81.5(6)			O5–Cu5–O6	80.4(6)
Cu3–O3	1.983(15)	O1–Cu2–O4	175.2(8)	Cu6–O7	1.957(15)	O5–Cu5–O8	175.2(7)
Cu3–O4	1.944(18)	O2–Cu2–O4	97.1(7)	Cu6–O8	1.974(18)	O6–Cu5–O8	96.1(7)
Cu3–N3	1.98(2)	O3–Cu2–O4	81.1(6)	Cu6–N7	1.99(2	O7–Cu5–O8	81.4(6)
Cu3–N4	1.94(2)	Cu2–O3–Cu3	91.9(6)	Cu6–N8	1.98(2)	Cu5–O7–Cu6	91.2(6)
Cu3–Br2	2.764(4)	Cu2–O4–Cu3	92.0(8)	Cu6–Br4	2.785(4)	Cu5–O8–Cu6	90.5(7)
		Cu1–Cu2–Cu3	179.61(15)			Cu4–Cu5–Cu6	179.58(15)
Cu1···Cu2	2.823(5)	O3–Cu3–O4	80.8(6)	Cu4···Cu5	2.814(5)	O7–Cu6–O8	82.5(6)
Cu2···Cu3	2.821(5)	N3–Cu3–N4	100.9(7)	Cu5···Cu6	2.817(5)	N7–Cu6–N8	101.2(7)
		O3–Cu3–N3	86.9(6)			O7–Cu6–N7	86.2(7)
Cu1···Br4$^{(ii)}$	3.193(4)	O3–Cu3–N4	161.4(8)	Cu4···Br2$^{(iv)}$	3.188(4)	O7–Cu6–N8	162.8(8)
Cu2···Br3$^{(i)}$	3.091(5)	O4–Cu3–N3	163.2(8)	Cu5···Br1	3.083(4)	O8–Cu6–N7	164.0(8)
Cu2···Br4$^{(ii)}$	3.080(4)	O4–Cu3–N4	87.7(7)	Cu5···Br2$^{(iv)}$	3.089(4)	O8–Cu6–N8	86.9(6)
Cu3···Br3$^{(i)}$	3.191(4)	O3–Cu3–Br2	103.5(5)	Cu6···Br1	3.184(4)	O7–Cu6–Br4	103.0(5)
		Cu2–Cu3–Br2	127.80(14)			Cu5–Cu6–Br4	127.56(14)

[a] Symmetry operations for **1**: (i) = $1 - x, 1 - y, -z$, (iii) = $x, 0.5 - y, -0.5 + z$. Symmetry operations for **3**: (i) = $1 + x, y, z$; (ii) = $x, -1 + y, z$; (iv) = $-1 + x, 1 + y, z$.

Table 2 Interlayer spacing from X-ray powder diffraction of the compounds **1–6** with R as a protruding residue of the amino alcoholate[a]

Compound	R	Inter layer spacing in Å
1	H	8.48
2	Me	10.24
3	Et	12.15
4	Ph	15.88
5	H	8.50
6	Et	12.26

[a] R = H, amino-ethanolate (ae, **1**, **5**); R = Me, (*R*)-2-amino-propan-1-olate (ap, **2**); R = Et, (*R*)-2-amino-butan-1-olate (ab, **3**, **6**); R = Ph, (*R*)-2-amino-2-phenyl-ethanolate (aPhe, **4**).

ligands chelate the two outer square-pyramidal Cu atoms (τ = 0.007 for **1**, τ = 0.02–0.04 for **3**).[44] For achiral compound **1** the middle square-planar Cu atom sits on an inversion center (Fig. 1a). The inversion symmetry is absent for the non-centrosymmetric structure of the enantiopure compound **3**, where two crystallographically independent trinuclear SBUs form the asymmetric unit (Fig. 1b).

The extended packing of the two very similar structures **1** and **3** is discussed for compound **1**. Inter-SBU Jahn–Teller Cu···Br contacts extend the coordination sphere of the Cu atoms to tetragonal bipyramidal with two different axial Cu–Br distances for Cu1 (Fig. 2a) and identical Cu–Br distances by symmetry for the central Cu2 (Fig. 2b). These charge-assisted $Cu^{(2+)}\cdots^{(-)}Br$ contacts connect the neutral trinuclear copper SBUs of **1** and **3** (*cf.* Fig. 1) to 2D sheets (Fig. 3a). The inter-SBU-{Cu···Br}-interactions are reinforced through charge-assisted N–H···$^{(-)}$O and N–H···$^{(-)}$Br hydrogen bonds (Fig. 3b).[41,43,45]

The packing diagrams of compounds **1** and **3** in Fig. 4 illustrate the lamellar or layer-like packing of hydrophobic and hydrophilic regions. The charge-assisted interactions are situated within the layer, while between adjacent layers only van-der-Waals interactions take place. The trinuclear amino alcoholate metal complexes appear to have a propensity for layer packing. We interpret the layer packing as being a consequence of the stronger charge-assisted Cu···Br and hydrogen-bonding interactions between the polar hydrophilic parts of the trinuclear SBUs. Crystal growth is favored along these strong supramolecular interactions,[41,43,45] that is, along

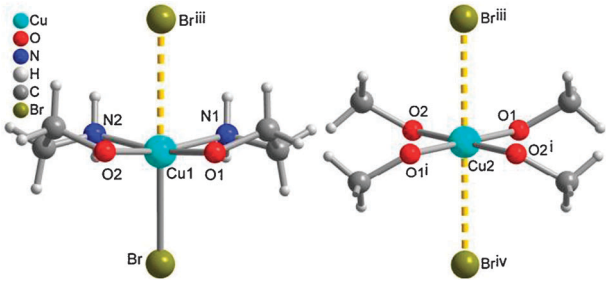

Fig. 2 Coordination spheres with charge-assisted $Cu^{(2+)}\cdots^{(-)}Br$ contacts in **1** for (left) Cu1 and (right) Cu2 (only the alkoxy group shown for clarity). Symmetry operations: (i) = $1 - x$, $1 - y$, $-z$; (iii) = x, $0.5 - y$, $-0.5 + z$; (iv) = $1 - x$, $0.5 + y$, $0.5 - z$.

the layer. These charge-assisted interactions are clearly seen as the driving force of the layer formation and expose the hydrophobic alkyl groups to the exterior (Scheme 3). We call such a layer with a hydrophilic interior and hydrophobic exterior a "hydrophobic-exterior layer".[46] The weak van-der-Waals

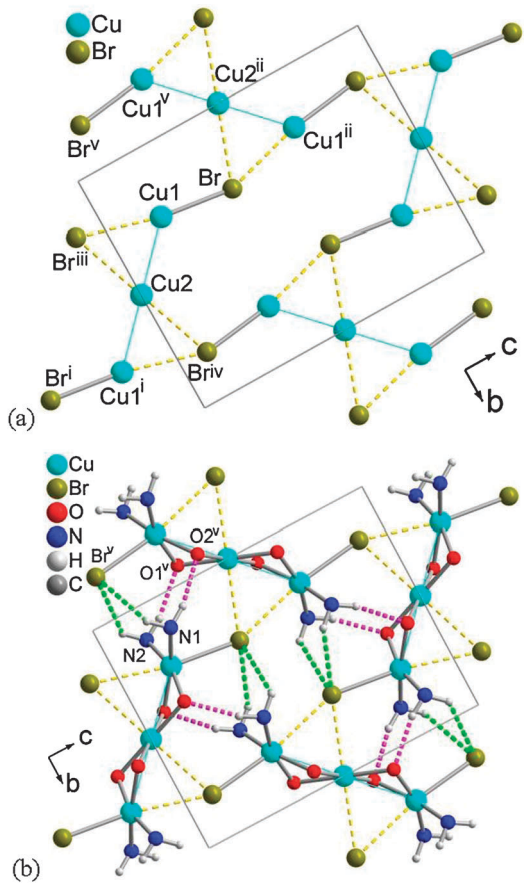

Fig. 3 2D-layer in **1** (and similarly in **3**) showing (a) charge-assisted $Cu^{(2+)}\cdots^{(-)}Br$ contacts depicted as dotted yellow lines (amino alcoholate ligands omitted for clarity) and (b) additional charge-assisted $N–H\cdots^{(-)}O$ (pink) and $N–H\cdots^{(-)}Br$ (green) hydrogen bonds (C-atoms are omitted for clarity). Cu···Br-distances and topological Cu–Cu contacts in Table 1; H-bond distances and angles in Table S1 in ESI.† Symmetry transformations: (i) = $1 - x$, $1 - y$, $-z$; (ii) = x, $0.5 - y$, $0.5 + z$; (iii) = x, $0.5 - y$, $-0.5 + z$; (iv) = $1 - x$, $0.5 + y$, $0.5 - z$; (v) = $x + 1$, $y - 0.5$, $-z + 0.5$.

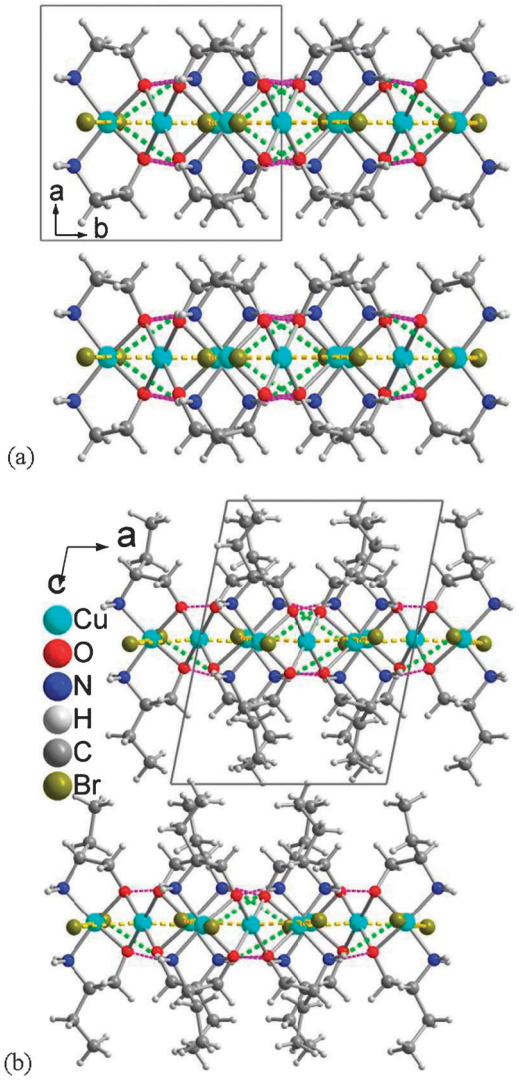

Fig. 4 Packing diagram of (a) **1** and (b) **3** with $N–H\cdots^{(-)}O$ and $N–H\cdots^{(-)}Br$ hydrogen bonds indicated as pink and green dashed lines, respectively. For packing diagrams with other viewing directions see Fig. S11 in ESI.†

interactions between the hydrophobic-exterior regions of adjacent layers then lead to the crystallization of thin plates for compounds **1–6**. Face-indexing could not be carried out, due to the poor visibility along the thin dimension of the plate. However, it is safe to assume that the plane of the thin crystals corresponds to the *bc*-plane with the *a*-axis orthogonal to the thin dimension in **1** and to the *ac*-plane with the *c*-axis orthogonal in **3**. Thus, the vertical *a*- and *c*-axes in Fig. 4 can be taken as the stacking directions for the hydrophobic-exterior layers (Scheme 3).

The powder diffractograms of compounds **1** to **6** (Fig. S1–S5 in ESI†) show a high intensity peak between 2θ = 4–11°. From this peak the interlayer spacing can be deduced[47] and is given in Table 2. It is obvious that with larger substituents on C2 of the 2-amino alcohol (R═H, Me, Et, Ph) the interlayer spacing increases. The layer structure and connectivity within **1–6** are similar to the trinuclear layer structure $2D\text{-}\{(Cu_3(\mu\text{-ae})_2(\mu\text{-}N_3)_2)(\mu_3\text{-}N_3)_2\}$.[5]

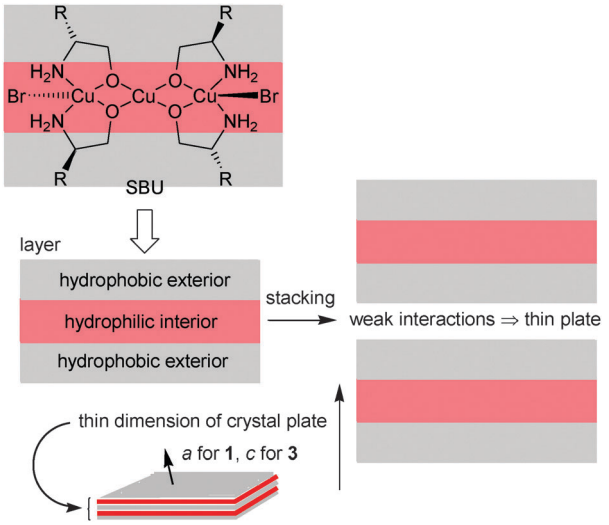

Scheme 3 Hydrophobic-exterior layer formation and stacking with weak "hydrophobic" van-der-Waals interactions to a thin crystal plate.

1D coordination polymers with mono and dinuclear SBUs

From the mother liquors of compounds **3** and **6**, that is, at lower concentrations, compounds 1D-[{Cu_2(μ-ab)$_2Br_2$}$_2$-{(μ$_3$-Br)Cu(abH)$_2$Br}{(μ$_3$-Br)Cu(abH)(CH_3OH)Br}] (**7**) and 1D-[{Cu_2(μ-ab)$_2Cl_2$}$_2${(μ$_3$-Cl)Cu(abH)(CH_3CH_2OH)Cl}$_2$] (**8**), respectively, crystallised. Compound **7** formed long dark green needles which are not stable outside the mother liquor, probably due to loss of coordinated methanol. Compound **8** formed light green needles upon solvent evaporation. Both needle crystals of **7** and **8** diffracted very poorly ($2\theta < 20°$) when exposed to the beam in a 90° angle to the needle. Therefore, the measuring strategy was adapted accordingly. However, the X-ray data are still of insufficient quality and only suitable for a better understanding of the concentration dependence and the different possibilities to form complexes from Cu(II), halide and amino alcohol ligands. Isostructural compounds **7** and **8** contain both mono and dinuclear SBUs assembled in chains.

Both structures of **7** and **8** contain four different and crystallographically independent SBUs, which are shown in Fig. 5 and S12 (ESI†), respectively. The neutral dinuclear SBUs correspond to those depicted in Scheme 1.[25–30] The two similar dinuclear SBUs encompass two copper atoms, two (*R*)-2-amino-butan-1-olate and two bromido (**7**) or chlorido (**8**) ligands (Fig. 5a and b). The Cu atoms are bridged by the deprotonated alcoholate oxygen atoms. The Cu atoms are distorted square-pyramidal coordinated when the charge-assisted $Cu^{(2+)}\cdots^{(-)}$Br/Cl contacts to neighboring mononuclear SBUs are included (Fig. 5a and b, S12 (ESI†)). The other two SBUs are neutral mononuclear units (Fig. 5c and d, S12 (ESI†)). In one the Cu atom is coordinated as a Jahn–Teller distorted octahedron by two bromide atoms and two amino alcohols (Fig. 5c). In the other mononuclear SBU the Cu atom is coordinated with one amino alcohol molecule, one solvent molecule (MeOH) and two bromide anions in distorted square-pyramidal geometry (Fig. 5d). All four SBUs are connected to a 1D coordination polymer through charge-assisted $Cu^{(2+)}\cdots^{(-)}$Br/Cl contact interactions (Fig. 6) supplemented by

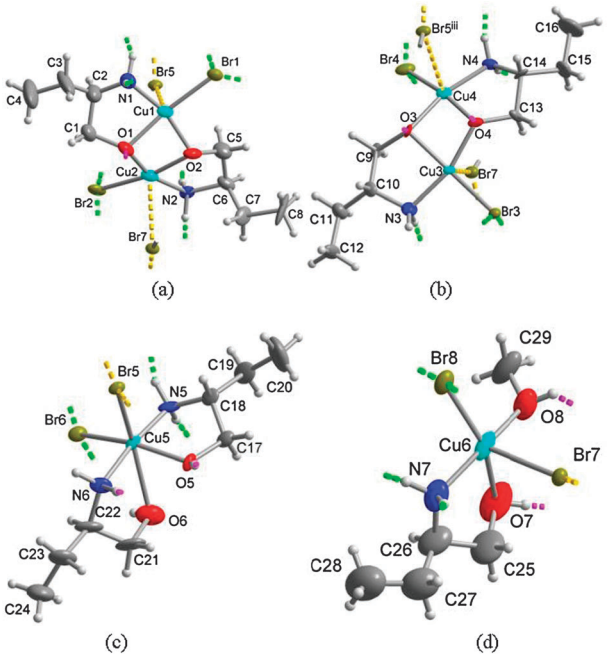

Fig. 5 (a) and (b) Dinuclear and (c), (d) mononuclear SBUs of compound **7** (30% thermal ellipsoids); charge-assisted $Cu^{(2+)}\cdots^{(-)}$Br (dashed yellow lines), N–H$\cdots^{(-)}$O (pink) and N–H$\cdots^{(-)}$Br (green) contacts are indicated; symmetry operation: (iii) = *x*, 1 + *y*, *z*; distances and angles in Table S2 (ESI†).

charge-assisted O–H$\cdots^{(-)}$O and N–H$\cdots^{(-)}$Br/Cl hydrogen bonds which then lead to supramolecular 2D layers (Fig. S13–S15 in ESI†). This way compounds **7** and **8** form a layer structure as compounds **1** and **3**, with the polar part shielded to both sides by the unpolar organic residues giving again "hydrophobic-exterior layers" with weak interlayer van-der-Waals packing (Fig. 7).

The structure of [$Cu(aeH)_2X_2$][$Cu_2(ae)_2X_2$] (with X = Cl or Br)[48] with both a dinuclear [$Cu(ae)_2X_2$] and a mononuclear [$Cu(aeH)_2X_2$]

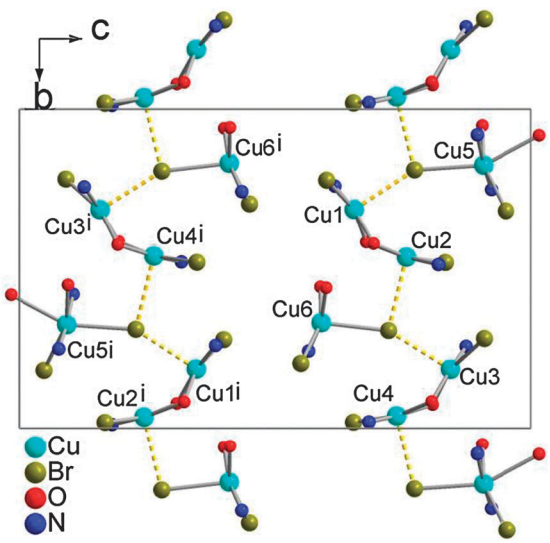

Fig. 6 1D strands in **7** through charge-assisted $Cu^{(2+)}\cdots^{(-)}$Br interactions (yellow dotted lines); C and H atoms are not shown for clarity; symmetry transformation: (i) = 1 − *x*, −0.5 + *y*, 1 − *z*; for the coexisting H-bonds see Fig. S13 and S14 in ESI.†

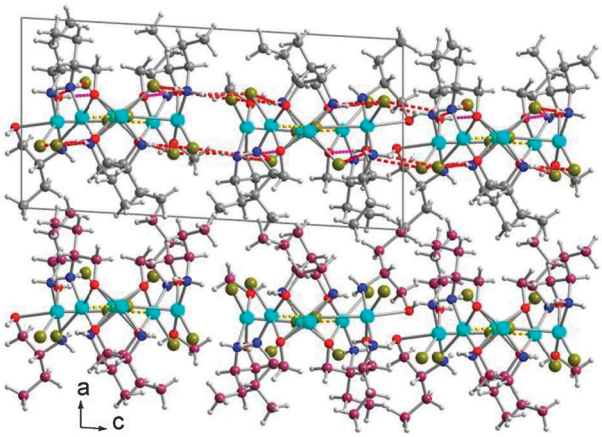

Fig. 7 Packing diagram of **7** and with N–H···$^{(-)}$O and N–H···$^{(-)}$Br hydrogen bonds indicated as red dashed lines in the top layer. C atoms of the bottom layer are represented by plum color for better discrimination between the two layers. For an additional packing diagram with another viewing directions see Fig. S16 in ESI.†

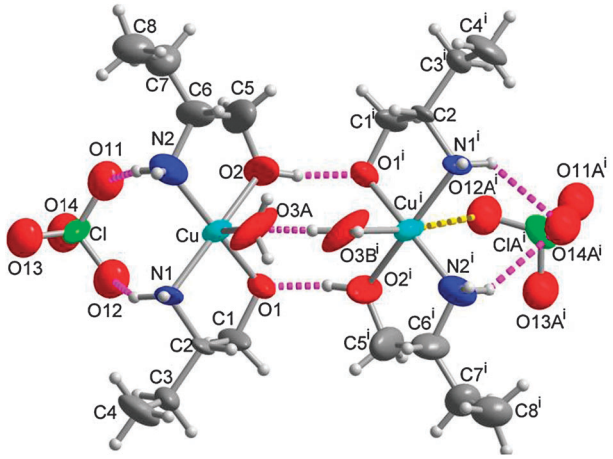

Fig. 8 Dimeric unit in **9** (50% thermal ellipsoids). The right moiety shows the Cu-coordinated orientation of the perchlorate anion (occupancy 50%). Each moiety shows one of the disordered aqua ligand orientations which determine each other; symmetry operation: (i) = $-x + 1, -y + 1, z$. Distances and angles are given in Table S3 and S4 in ESI.†

unit and the amino-ethanol/-ate (aeH/ae) ligand was reported as the result of a multi-step synthesis. Comparing structures **1–6** to **7** and **8** shows that several coordination modes are possible depending on the metal–ligand concentration and the ratio. The different building units appear to be in equilibrium with each other in solution judging from gradual color changes in the reaction solutions for single-crystal preparation (Fig. S17, ESI†) and in solutions with different Cu-to-amino alcohol ratios (Fig. S18 in ESI†).

Dimeric copper complex

Compound $\{[Cu(rac\text{-abH})(rac\text{-ab})H_2O]ClO_4\}_2$ (**9**) was isolated in an attempt to synthesize a Cu-amino alcoholate compound in which the SBUs are further connected through a bridging ligand (here terephthalate). The copper cation is coordinated in a square pyramid by one amino alcohol and one alcoholate ligand of each enantiomer and a disordered water molecule. Compound **9** consists of dimeric units, which form through head-to-tail hydrogen bonds between the alcohol and alcoholate ligands of two Cu complexes (Fig. 8). In 50% of the cases the perchlorate anion assumes a Cu-coordinating orientation.

Further charge-assisted H-bonds between the amino protons and the perchlorate anion and between the aqua ligands and the alcoholate oxygen atoms connect the dimeric units to a supramolecular 1D-strand along the *c*-axis (Fig. S19 in ESI†).

Magnetic properties of 1 and 3

Magnetic susceptibility measurements. The temperature dependence of the $\chi_M T$ product for compounds **1** and **3** is shown in Fig. 9a and b, respectively (χ_M is the magnetic susceptibility per three copper(II) ions).

At room temperature, $\chi_M T$ is 1.48 and 1.51 cm^3 mol^{-1} K, for **1** and **3**, respectively. These values are higher than those expected for three magnetically isolated copper(II) ions ($\chi_M T = 3(N\beta^2 g^2/3kT)\ S(S + 1) = 1.24$ cm^{3}mol^{-1} K, with $g = 2.1$ and $S = 1/2$).[49] $\chi_M T$ continuously increases on lowering the temperature and reaches maximum values of *ca.* 1.80 and 1.84 cm^3 mol^{-1} K at about 40 K for **1** and **3** respectively. The values of $\chi_M T$ decrease at lower temperatures. The features of the $\chi_M T$ *vs.* temperature plots are indicative of the occurrence of ferromagnetic and antiferromagnetic couplings in both compounds. At temperatures lower than 3 K the $\chi_M T$ product of compound **1** increases abruptly; this behavior is characteristic of an onset of long-range magnetic ordering at that temperature. The magnetic ordering is more likely due to intermolecular interactions through the bromide ions that connect the copper(II) trinuclear units and give rise to a long range interaction. Due to the antiferromagnetic nature of the intermolecular interactions the long-range magnetic ordering arises from a canted antiferromagnetism. AC magnetic measurements were performed in the 1.9 to 5 K interval at different frequencies of the applied magnetic field (1 to 10 000 Hz); however, non-zero values for the out-of-phase signal were not observed, which means that the long-range magnetic ordering is achieved at lower temperatures.

For temperatures above 3 K and 2 K, for **1** and **3** respectively, the magnetic susceptibility data were analyzed by means of the general zero-field spin Hamiltonian for a linear trinuclear system

$$\hat{H} = -J\,(\hat{S}_1\hat{S}_2 + \hat{S}_2\hat{S}_3) - j(\hat{S}_1\hat{S}_3) \qquad (1)$$

where J refers to the exchange coupling between the central and terminal Cu(II) ions and j to the exchange between the two terminal Cu(II) ions. Compound **3** contains two slightly different trinuclear units, but the copper(II) ions are bridged by the same atoms and the structural parameters are so similar that the compound can be studied by means of the spin Hamiltonian shown in eqn (1). This Hamiltonian can be easily solved, making $\hat{S}_A = \hat{S}_1 + \hat{S}_3$ and $\hat{S}_T = \hat{S}_2 + \hat{S}_A$ and for three spin doublets ($S_1 = S_2 = S_3 = 1/2$) it gives rise to three different spin states, a quartet ($S_T = 3/2$) and two doublets ($S_T = 1/2$), which arise from the different $S_A = 1, 0$ spin intermediates. The energy $E_{|ST,SA\rangle}$ of the eigenvalues is $E_{|3/2,1\rangle} = -3J/2$, $E_{|1/2,0\rangle} = -\delta$ and $E_{|1/2,1\rangle} = 0$, with $\delta = J - j$.[49,50]

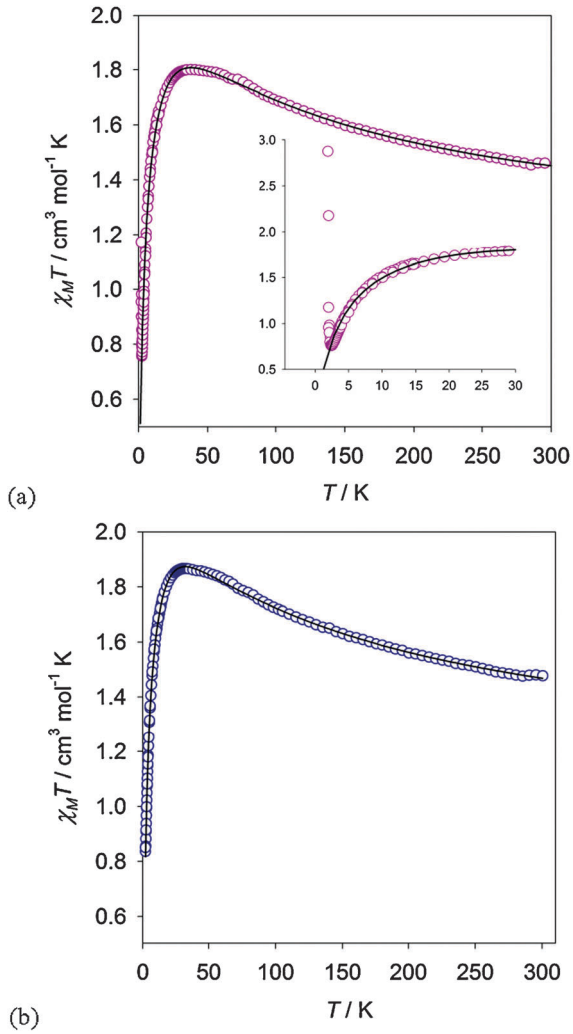

Fig. 9 Temperature dependence of the $\chi_M T$ product for compounds **1** (a) and **3** (b), respectively. The solid line corresponds to the best fit to eqn (3) (see text). The inset in (a) shows the same data, but in the low temperature region.

The numerical expression for the magnetic susceptibility is then

$$\chi_{\text{trinucl}} = \frac{N\beta^2 g^2}{4kT}\left[\frac{1+\exp{}^{\delta}/_{kT}+10\exp{}^{3J}/_{2kT}}{1+\exp{}^{\delta}/_{kT}+2\exp{}^{3J}/_{2kT}}\right] \qquad (2)$$

where N is Avogadro's number, β the Bohr magneton, k the Boltzmann constant and g the mean Landé factor. Considering that a ferromagnetic coupling is observed, a term for the zero-field splitting between the $\pm 3/2$ and $\pm 1/2$ Kramer doublets coming up from the $S = 3/2$ state could also be included in the Hamiltonian. However, the value of the zero-field splitting D, cannot be accurately calculated for copper(II) trinuclear systems from magnetic susceptibility measurements in polycrystalline samples and in most cases this term is discarded.[49,51,52] On the other hand, as has been mentioned, the bromide ions interconnect the different trinuclear units and the intermolecular interactions play an important role in the magnetic behaviour of these compounds. Therefore, these intermolecular interactions

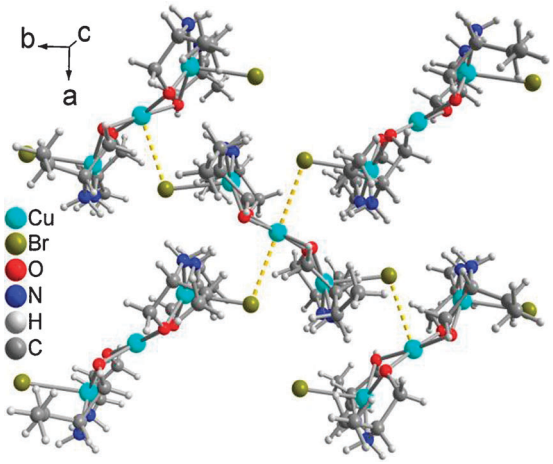

Fig. 10 Intermolecular interactions through the bromide ion in **3** (and similarly in **1**). The central trinuclear unit interacts with its four nearest neighbors through the bromide ions (*cf.* Fig. 3).

are taken into account with the molecular field approximation

$$\chi = \chi_{\text{trinucl}} \Big/ \left[1 - \left(\frac{zj'\chi_{\text{trinucl}}}{N\beta^2 g^2}\right)\right] \qquad (3)$$

where j' corresponds to the intermolecular coupling amongst the trinuclear units and $z = 4$, since each trinuclear unit has four neighbors around it (see Fig. 10). With this model the intermolecular antiferromagnetic couplings are responsible for the decrease in the $\chi_M T$ product at low temperatures. Noteworthy that the values found for j' must be viewed as upper limits since the single ion anisotropy exhibits the same effect.

Under this approach the magnetic susceptibility data were analyzed by means of eqn (2) and (3) and the best fit parameters are shown in Table 3. It can be observed that the compounds exhibit a ferromagnetic coupling between the central and the two terminal copper(II) ions whereas an antiferromagnetic coupling is observed between the two terminal copper(II) ions. The calculated curves are a good match to the data in the temperature range studied ($R = \sum_i[(\chi_M T)_{\text{obs}}(i)-(\chi_M T)_{\text{calc}}(i)]^2/\sum_i[(\chi_M T)_{\text{obs}}(i)]^2$).

The magnetic behaviour of alkoxo-bridged copper(II) dinuclear and linear trinuclear complexes has been the subject of previous studies. According to the literature, the key parameters governing the magnetic behaviour of these compounds are (i) the Cu–O–Cu angle of the μ-alkoxo bridge (φ), (ii) the Cu···Cu distance, (iii) the out-of-plane shift of the carbon atom of the alkoxo bridge (τ) and (iv) the hinge distortion of the $[Cu_2(\mu_2\text{-}O)_2]$ core (γ).[49,53–56] Nevertheless, the Cu–O–Cu angle, in most cases, is able to explain the values and the trend of the values of the magnetic coupling constants for those compounds. Hatfield and Hodgson found a linear correlation between the experimentally determined exchange coupling constant and the Cu–O–Cu bond angle (φ).[54] They found antiferromagnetic behavior for complexes with φ larger than 97.6°, whereas ferromagnetism appears for those with smaller values of φ. An apparently similar linear relationship is observed for the alkoxo-bridged copper(II) complexes at angles around 95.6°.[56,57] Some magnetic and structural parameters of representative compounds are shown in Table 3 with those of

Table 3 Magnetic parameters and mean Cu–O–Cu angles of compounds **1** and **3** and other alkoxo-bridged copper(II) dinuclear and trinuclear complexes exhibiting ferromagnetic and antiferromagnetic couplings

Compound	Cu–O–Cu/°	J/cm^{-1}	j/cm^{-1}	j'/cm^{-1}	g	$R \times 10^5$	Ref.
1	91.12(20)	139(2)	−15(1)	−0.55(1)	2.11(1)	3.50	This work
3	91.5(8)	145(2)	−25(2)	−0.45(1)	2.14(1)	2.12	This work
A	91.31(15)	153(2)			2.13(1)		53[a]
B	95.92	118(2)			2.02(1)		53[a]
C	96.26(5)	94.9(6)			2.16(1)		53[a]
D	98.35	−314.0(8)		−0.50(1)	2.09	0.15	56[b]
E	98.72	−482(3)		−1.2(1)	2.17(1)		58[b]
F	101.36	−303(1)		−2.1(2)	2.24(1)		58[b]
G	99.55	−474(3)		−0.08(3)	2.02(0)		59[b]

[a] Alkoxo-bridged dinuclear complexes. [b] Alkoxo-bridged trinuclear complexes. **A** = $[Cu_2(Hmdea)_2(\mu\text{-}H_2O)(\mu_2\text{-tpa})]_n$, **B** = $[Cu_2(H_2tipa)_2(\mu_2\text{-ipa})]_n$, **C** = $[Cu_2(H_2tea)_2(\mu_2\text{-tpa})]_n$, **D** = $[Cu_3(\mu\text{-L})_2](CH_3OH)_2(ClO_4)_2$, **E** = $[Cu_3(bhbd)_2Cl_2](CH_3OH)_4$, **F** = $[Cu_3(bhbd)_2(CH_3OH)_4(ClO_4)_2]$, **G** = $[Cu_3(bhdh)_2(MeCN)_2I_2](MeCN)_2$, H_2mdea: methyldiethanolamine, H_3tipa: triisopropanolamine, H_3tea: triethanolamine, ipa: isophthalic acid, H_2tpa: terephthalic acid, H_2L: *N,N′*-bis(2-hydroxybenzyl)-1,4-diazacycloheptane, H_2bhbd: bis(2-hydroxybenzyl)-1,3-diaminopropane, H_2bhdh: 1,7-bis(hydroxyphenyl)-2,6-diaza-4-hydroxyl-heptane.

compounds **1** and **3**. All di-μ-alkoxo bridged copper(II) linear trinuclear complexes reported display antiferromagnetic couplings with large Cu–O–Cu angles[56,58–60] and for comparison purposes ferromagnetically-coupled di-μ-alkoxo bridged copper(II) dinuclear complexes[53] have been included in Table 3. It can be observed that the general trend is followed and the ferromagnetic coupling observed in compounds **1** and **3** is in agreement with their structural parameters.

DFT calculations

In some cases copper(II) linear trinuclear complexes are satisfactorily studied with this zero-field spin Hamiltonian[5,52,56,58]

$$\hat{H} = -J(\hat{S}_1\hat{S}_2 + \hat{S}_2\hat{S}_3) \quad (4)$$

which considers only couplings between the central and the terminal copper(II) ions, discarding the interactions between the two terminal copper(II) ions ($j = 0$ in eqn (1)). Our approach is more general, since, in principle, it does not reject this latter interaction that has also been observed in other linear trinuclear systems.[61] Nevertheless, in order to check if our model is the best model to describe the magnetic behavior of compounds **1** and **3**, DFT broken symmetry calculations have been performed to calculate the values of the J and j coupling constants. The calculation details are given in the experimental section. This method allows to determine n different magnetic coupling constants by knowing the energy of $n + 1$ spin configurations.[61] For the case of copper(II) trinuclear complexes three different spin configurations can be found: the high spin, with a total spin of 3/2, and two doublets, with total spin $\frac{1}{2}$. The spin distributions in the three configurations can be seen in Scheme 4.

The relative energies of the three spin configurations are shown in Fig. 11. It can be seen that the ground state is the 3/2 state in which all the spins are parallel (↑↑↑). The state with higher energy is the symmetric $\frac{1}{2}$ state in which an alternation of the spins takes place (↑↓↑). This result is consistent with the ferromagnetic nature of both compounds.

The values of the magnetic coupling constants can be calculated from the energy of those spin configurations by the following equations:

$$E_{HS} - E_{LS1} = -2J \quad (5)$$

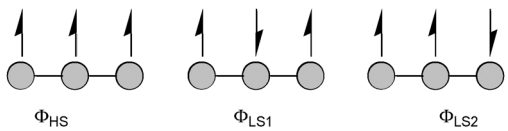

Scheme 4 Spin distributions for which the energy has been calculated.

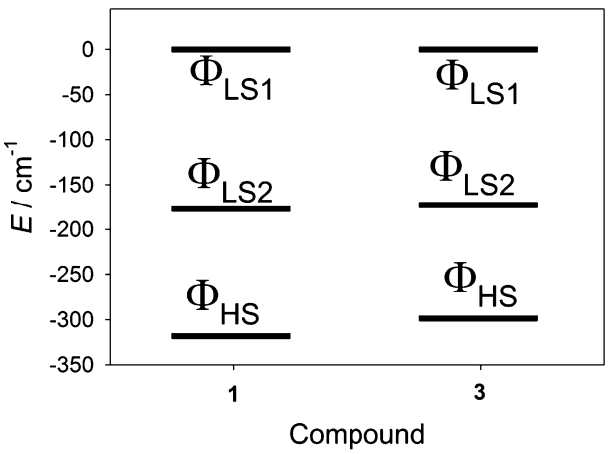

Fig. 11 Energy diagram of the different spin distributions of compounds **1** and **3**. The ground state for both compounds has spin 3/2.

$$E_{HS} - E_{LS2} = -J - j \quad (6)$$

where E_{HS}, E_{LS1} and E_{LS2} correspond to the energy of the high spin and the two broken symmetry low spin states.[61,62] The results are shown in Table 4 and compared to those calculated from the magnetic susceptibility measurements.

A very good agreement is observed between the experimental and theoretical magnetic coupling constants. From this study we can conclude that the interaction between the terminal copper(II) ions in these linear trinuclear systems is operative and cannot be neglected and that the model selected for the analysis of the data is the correct one.

Conclusions

Enantiopure trinuclear Cu-amino alcoholate SBUs $\{Cu_3(\mu\text{-L})_4X_2\}$ can be reproducibly obtained from Cu(II) halides, CuX_2 in the

Table 4 Experimental and calculated magnetic coupling constants in cm^{-1} for compounds **1** and **3**

Compound	Exp. J	Calc. J	Exp. j	Calc. j
1	139(2)	159.0	–15(1)	–18.1
3	145(2)	149.2	–25(2)	–23.6

presence of base for the deprotonation of the enantiopure amino alcohol LH. Supramolecular interactions then aggregate the SBU into "hydrophobic exterior" layers with a polar hydrophilic interior and unpolar groups oriented away to both sides. The stacking of the hydrophobic-exterior layers occurs through van-der-Waals interactions between the alkyl or aryl groups. Because of the general weakness of this type of interaction crystal growth along this stacking direction does not proceed well. Thus, thin crystal plates form along the charge-assisted $Cu^{(2+)}\cdots^{(-)}Br$, $N–H\cdots^{(-)}O$ and $N–H\cdots^{(-)}Br$ bond orientation.[41,43,45]

A magnetic study for the structurally elucidated compounds **1** and **3** shows a ferromagnetic coupling which is in agreement with their structural parameters, mainly the Cu–O–Cu bond angle. A very good agreement for $\{Cu_3(\mu\text{-}L)_4X_2\}$ between the experimental and theoretical magnetic J,j coupling constants indicates that an interaction between the terminal copper(II) ions in these linear trinuclear systems is operative.

Experimental

General

Materials. Reagents and solvents were obtained from commercial sources and were used without further purification: $Cu(ClO_4)_2{\cdot}6H_2O$ (Aldrich), anhydrous $CuBr_2$ (ABCR), $CuCl_2$ (Aldrich), (*R*)-amino-2-propanol (Fluka), (*R*)-2-amino-1-butanol (AlfaAesar), (*R*)-2-phenylglycinol (AlfaAesar), amino-ethanol (Aldrich), triethylamine, TEA (synthesis grade Roth), methanol and ethanol (synthesis grade Roth).

Physical measurements. Elemental analyses for C, H, and N were performed with a Perkin Elmer CHN 2400 Series 2. IR spectra were recorded on a Nicolet Magna-IR 760 equipped with a Diamond ATR unit. Medium IR (MIR) was measured from 4000 to 400 cm^{-1} and far IR (FIR) from 600 to 100 cm^{-1}. The following abbreviations were used to classify spectral bands: br (broad), sh (shoulder), very weak (vw), w (weak), m (medium), s (strong), vs (very strong).

Powder X-ray diffraction patterns were measured at ambient temperature using a STOE STADI-P with a transmission image-plate, Cu-Kα radiation (λ = 1.54 Å), a Ge(111) monochromator and stationary flat panel samples. Simulated powder patterns were based on single-crystal data and calculated using the STOE WinXPOW software package.[63]

Magnetic susceptibility measurements on polycrystalline samples were carried out by means of a Quantum Design SQUID MPMS XL magnetometer. The DC measurements were performed in the temperature range 1.9–300 K at applied magnetic fields of 100 Oe for $T < 15$ K, and 1000 Oe for $T > 10$ K. Diamagnetic corrections of the constituent atoms were estimated from Pascal's constants[49] and experimental susceptibilities were also corrected for the temperature-independent paramagnetism and the magnetization of the sample holder.

General synthesis procedure for bulk material of compounds 1–4 and 6

A solution of anhydrous CuX_2 [X = Br (**1** to **4**), X = Cl (**5**, **6**)] in methanol (2 mL) was added to a combined solution of the amino alcohol LH and TEA in methanol (5 mL). The blue product precipitate was filtered, washed with methanol (3 × 3 mL) and Et_2O (10 mL) and dried in air. The yield was quantitative with respect to CuX_2.

2D-[$Cu_3(\mu\text{-ae})_4(\mu_3\text{-Br})_2$] (1)

0.11 g (0.50 mmol) $CuBr_2$, 0.042 g (0.69 mmol) aeH and 0.084 g (0.83 mmol) TEA. Yield 0.096 g. $C_8H_{24}Br_2Cu_3N_4O_4$ (590.75) calc. 16.27, H 4.09, N 9.48; found C 16.25, H 4.07, N 9.22%. IR: FIR (ATR) ν/cm^{-1} = 89.3 (vs), 100.1 (s), 113.8 (s), 168.9 (s), 181.2 (w), 226.9 (m), 288.9 (vs), 376.9 (s), 430.0 (s), 494.6 (s), 589.7 (m); MIR (ATR) ν/cm^{-1} = 430.0 (vs), 494.3 (vs), 589.6 (s), 698.2 (vs), 887.3 (s), 1007.9 (s), 1058.7 (vs) 1116.3 (w), 1194.3 (w), 1256.4 (w), 1290.8 (w), 1352.6 (m), 1376.0 (w), 1455.7 (w), 1587.8 (vs), 2686.7 (w), 2834.2 (m), 2853.4 (m), 2920.0 (w), 2938.7 (w), 3114.4 (m), 3201.4 (m), 3277.5 (m).

2D-[$Cu_3(\mu\text{-}R\text{-ap})_4(\mu_3\text{-Br})_2$] (2)

0.103 g (0.46 mmol) $CuBr_2$, 0.046 g (0.61 mmol) apH and 0.066 g (0.65 mmol) TEA. Yield 0.097 g. $C_{12}H_{32}Br_2Cu_3N_4O_4$ (646.85) calc. 22.28, H 4.99, N 8.66; found C 21.82, H 4.96, N 8.37%. IR: FIR (ATR) ν/cm^{-1} = 82.7 (s), 103.3 (vs), 236.7 (m), 264.1 (s), 358.6 (m), 374.1 (s), 406.3 (m), 442.4 (s), 494.8 (m), 530.2 (m), 587.4 (m); MIR (ATR) ν/cm^{-1} = 441.9 (vs), 496.0 (m), 530.3 (m), 588.1 (m), 670.5 (s), 709.1 (m), 804.0 (w), 841.3 (w), 939.9 (w), 995.3 (s), 1061.1 (vs), 1110.6 (m), 1179.7 (w), 1229.7 (w), 1317.4 (w), 1381.2 (w), 1461.6 (w), 1585.1 (vs), 2702.6 (w), 2840.3 (m), 2862.4 (m), 2928.4 (w), 2958.7 (w), 3119.4 (m), 3206.0 (m), 3259.3 (m).

2D-[$Cu_3(\mu\text{-}R\text{-ab})_4(\mu_3\text{-Br})_2$] (3)

0.101 g (0.45 mmol) $CuBr_2$, 0.062 g (0.70 mmol) apH and 0.075 g (0.74 mmol) TEA. Yield 0.105 g. $C_{12}H_{32}Br_2Cu_3N_4O_4$ (702.96) calc. 27.34, H 5.74, N 7.97; found C 27.11, H 5.7, N 7.84%. IR: FIR (ATR) ν/cm^{-1} = 85.9 (s), 102.8 (s), 169.7 (m), 235.5 (m), 350.7 (m), 436.4 (m), 467.7 (m), 501.9 (m), 579.8 (m); MIR (ATR) ν/cm^{-1} = 436.2 (vs), 467.2 (s), 501.8 (m), 532.8 (w), 580.4 (m), 669.1 (s), 704.4 (m), 773.1 (m), 830.2 (w), 866.0 (w), 925.5 (w), 1025.1 (s), 1063.7 (vs), 1114.6 (m), 1161.6 (w), 1308.8 (w), 1342.4 (w), 1381.9 (w), 1461.3 (m), 1582.4 (vs), 2854,1 (s), 2874.4 (m), 2928.6 (w, br), 2958.8 (m), 3118,1 (w), 3209.1 (m), 3261.3 (w).

2D-[$Cu_3(\mu\text{-}R\text{-aPhe})_4(\mu_3\text{-Br})_2$] (4)

0.0674 g (0.3 mmol) $CuBr_2$, 0.0607 g (0.45 mmol) aPheH and 0.049 g (0.48 mmol) TEA. Yield 0.087 g. $C_{32}H_{40}Br_2Cu_3N_4O_4$ (895.13) calc. C 42.94, H 4.5, N 6.26; found C 42.95, H 4.45, N 6.24%. IR: FIR (ATR) ν/cm^{-1} = 96.9 (m), 114.5 (w), 134.6 (w), 173.0 (w), 224.8 (w), 352.5 (w), 395.7 (w), 439.5 (w) 474.7 (w), 525.0 (w); MIR (ATR) ν/cm^{-1} = 438.2 (s), 473.7 (s),

523.9 (s), 651.2 (s), 664.6 (s), 694.5 (vs), 751.0 (m), 842.2 (w), 910.4 (w), 1025.7 (s), 1047.3 (s), 1143.0 (w), 1187.5 (w), 1264.1 (w), 1376.7 (w), 1451.7 (m), 1495.2 (m), 1579.6 (s), 2856.7 (w), 2914.7 (w), 3029.2 (w), 3060.9 (w), 3117.8 (w), 3197.0 (m) (ZnS-unit additional peaks at 1800.3 (vw), 1871.6 (vw), 1943.0 (vw), 1858.9 (w)).

2D-[Cu_3(μ-ae)$_4$(μ$_3$-Cl)$_2$] (5)

A solution of 0.139 g (1.03 mmol) $CuCl_2$ in methanol (4 mL) was added to a solution of 0.091 g (1.49 mmol) aeH and 0.141 g (1.39 mmol) TEA in methanol (8 mL). The blue precipitate obtained was filtered and washed with methanol and Et_2O and left to dry. Yield 0.172 g, quantitative with respect to $CuCl_2$. $C_8H_{24}Cl_2Cu_3N_4O_4$ (501.84) calc. 19.15, H 4.82, N 11.16; found C 18.57, H 5.07, N 10.64%. IR: FIR (ATR) ν/cm^{-1} = 103.5 (vs), 117.8 (vs), 169.7 (s), 234.1 (w), 291.5 (s), 382.7 (s), 426.3 (m), 438.2 (m), 498.6 (m), 591.3 (w); MIR (ATR) ν/cm^{-1} = 426.0 (vs), 484.5 (s), 498.3 (s), 591.6 (m), 700.6 (s), 887.4 (m), 1007.5 (s), 1047.3 (vs), 1061.2 (vs), 1122.0 (w), 1195.2 (w), 1257.5 (w), 1291.6 (w), 1353.5 (w), 1376.1 (w), 1454.7 (w), 1591.2 (s), 2687.7 (w), 2834.6 (m), 2851.7 (m), 2871.7 (w), 2919.4 (w), 2937.5 (w), 3100.9 (m), 3198.3 (m), 3287.8 (m).

2D-[Cu_3(μ-*R*-ab)$_4$(μ$_3$-Cl)$_2$] (6)

0.101 g (0.45 mmol) $CuCl_2$, 0.062 g (0.70 mmol) apH and 0.075 g (0.74 mmol) TEA. Yield 0.152 g. $C_{12}H_{32}Cl_2Cu_3N_4O_4$ (614.06) calc. 31.30, H 6.57, N 11.16; found C 18.57, H 6.71, N 8.97%. IR: FIR (ATR) ν/cm^{-1} = 103.5 (vs), 117.8 (vs), 169.7 (s), 234.1 (w), 291.5 (s), 382 (m), 426.3 (m), 483.2 (m), 498.6 (m), 591.3 (w); MIR (ATR) ν/cm^{-1} = 432.3 (vs), 467.6 (s), 503.7 (m), 583.1 (m), 676.0 (s), 705.2 (m), 774.4 (m), 831.9 (w), 868.2 (w), 926.5 (w), 1021.5 (s), 1065.3 (vs), 1118.0 (m), 1164.4 (w), 1309.0 (w), 1382.7 (w) 1460.7 (m), 1587.8 (vs), 2853.6 (s), 2959.8 (m), 3114.9 (m), 3204.8 (m), 3271.3 (w).

Synthesis of single-crystalline materials of 1, 3, 7 and 8

Single-crystals of the four compounds were obtained by slow diffusion of reactants. The representative nature of the single crystals investigated by X-ray diffactometry and identity of the bulk samples of **1** and **3** were verified in all cases by positively matching the measured X-ray powder diffractograms of a larger crystal selection or from bulk samples with the diffractogram simulated from the data of the single-crystal X-ray refinement (see Fig. S1–S5 in ESI†). For photographs of the experimental setup see Fig. S16 in ESI.†

2D-[Cu_3(μ-ae)$_4$(μ$_3$-Br)$_2$] (1)

A small glass vial with 0.033 g (0.15 mmol) $CuBr_2$ was placed into a bigger glass vial containing 0.018 g (0.29 mmol) aeH. Both vials were carefully filled with methanol until the small vial was fully covered so that a connection for diffusion through the solvent was established (*ca.* 10 mL MeOH total). After two weeks the color of the solution was homogeneously green and blue crystals of **1** were collected for single crystal diffractometry from the top of the inner vial.

2D-[Cu_3(μ-*R*-ab)$_4$(μ$_3$-Br)$_2$] (3) and 1D-[{Cu_2(μ-ab)$_2$Br$_2$}$_2$-{(μ$_3$-Br)Cu(abH)$_2$Br}{(μ$_3$-Br)Cu(abH)(CH_3OH)Br}] (7)

A small glass vial with 0.038 g (0.17 mmol) $CuBr_2$ was placed into a bigger glass vial containing 0.0288 g (0.32 mmol) abH. Both vials were carefully filled with methanol until the small vial was fully covered so that a connection for diffusion through the solvent was established (*ca.* 10 mL MeOH). After one day, the solution had turned green with a colour gradient to the brown $CuBr_2$ solution on the bottom of the inner vial. After another week the color of the solution was homogeneously green and blue crystals of **3** were collected for single crystal diffractometry from the top outside edge of the inner vial.

After decanting, the green solution was left standing for slow evaporation. After four days very thin and long dark green needles had grown along the glass wall of the vial and were collected for single crystal diffractometry. Unfortunately, these green crystals did not represent a pure phase so no further analytical data were obtained.

1D-[{Cu_2(μ-ab)$_2$Cl$_2$}$_2${(μ$_3$-Cl)Cu(abH)(CH_3CH_2OH)Cl}$_2$] (8)

A small glass vial with 0.018 g (0.13 mmol) $CuCl_2$ was placed into a bigger glass vial containing 0.019 g (0.21 mmol) abH. Both vials were carefully filled with ethanol until a connection for diffusion through the solvent was established (*ca.*10 mL MeOH). After two weeks the color of the solution was homogeneously green with no crystals formed. The solution was left for slow evaporation and after five days very thin and long light green needles had grown at the edge of the solution and were collected for single crystal diffractometry. Again, these green needles did not represent a pure phase so no further analytical data were obtained.

{[Cu(*rac*-abH)(*rac*-ab)H_2O]ClO_4}2 (9)

A solution of 0.207 g (2.05 mmol) TEA and 0.187 g (2.10 mmol) *rac*-abH in 3 mL MeOH was mixed with 2 mL of a MeOH solution of 0.553 g (1.49 mmol) $Cu(ClO_4)_2{\cdot}6H_2O$. The dark blue solution was left in a closed vial. After one day blue crystals had grown and the solution color intensity had faded. Yield 0.423 mg (79%). $C_{16}H_{46}Cl_2Cu_2N_4O_{14}$ (716.55) calc. C 26.82, H 6.47, N 7.82; found C 26.72, H 6.16, N 7.75%. IR: MIR (ATR) ν/cm^{-1} = 429.1 (m), 619.1 (vs), 673.5 (m), 776.6 (m), 855.2 (m), 924.4 (s), 1031.2 (br, vs), 1164.8 (m), 1241.8m (m), 1304.5 (m), 1387.8 (m), 1440.4 (m), 1586.2 (m), 2881.8 (w), 2935.2, 2935.2 (w) 2967.4 (w), 3268.7 (w), 3326.6 (w).

X-Ray crystallography

Suitable single crystals were carefully selected under a polarizing microscope. Data collection: compounds **1**, **5**, **6** and **7** Bruker Apex II microsource, CCD Detector, Mo-Kα radiation (λ = 0.71073 Å), graphite monochromator, double-pass method ω-scan and φ-scan. Cell refinement with APEX2,[64] data reduction with SAINT.[65] Compound **3** Rigaku R-axis Spider image plate detector, Mo-Kα radiation (λ = 0.71073 Å), graphite monochromator, double-pass method ω-scan and φ-scan; data collection, cell refinement and data reduction with CrystalClear.[66] Due to twinning no experimental absorption correction was carried out. The crystals of **1** and **3** were very thin

blue square plates that easily split into even thinner plates. It was not possible to determine the thickness of the plates under the microscope. This crystal morphology was problematic for the X-ray diffraction measurements. Depending on the orientation of the crystal in relation to the X-ray beam, the crystals measured diffracted between $2\theta = 20°$ and $2\theta = 55°$; this had to be taken into account when the measuring strategy was developed for compound. Therefore, the crystal was placed carefully into the loop in such a way that in a 360° φ-scan the X-ray beam passed constantly through the diagonal. Two ω-scans with a sweep range of 202.5° (each with different 2θ settings) were used with a φ setting that ensured the crystal stayed with its plane parallel to the beam. Two more scans with settings calculated by COSMO, Bruker were added to get a better redundancy and completeness of the data. For compound **3** which was measured on the Rigaku the operator had little influence over the measurement strategy; furthermore, the crystal quality of **3** was poorer and severe twinning was observed. With heavy atoms such as copper and bromine in the structure of compound **3** and a crystal with such an anisotropic morphology (crystal size $0.15 \times 0.15 \times < 0.01$(!) mm^3) absorption artefacts are large. In addition the standard adsorption correction was not carried out on the raw data and only after the generation of the hkl5 file the built in adsorption correction of SHELX was undertaken during refinement. Also, bromine is known as a notoriously problematic atom in X-ray diffraction work with Mo-Kα radiation (*vide infra*). The crystal chosen for measurement (the best which could be found out of 15 attempts, from 3 different crystallisation attempts) still had three twin domains and data reduction was carried out without absorption correction to enable PLATON[67] to calculate the twin laws. PLATON was used to create a hklf5 file used for structure refinement. The TWIN law used to generate the hklf5 was

$$\begin{pmatrix} 1 & 0 & 0 \\ 0 & -1 & 0 \\ -0.5 & 0 & -1 \end{pmatrix} \begin{pmatrix} h \\ k \\ l \end{pmatrix} = \begin{pmatrix} h' \\ k' \\ l' \end{pmatrix}$$

However the structure of compound **3** is important for comparison with the structure of compound **1**. We can explain the origin of the high *R*-value (Table 5), hence, its significance as a quality parameter should be judged accordingly. All other crystallographic refinement values for compound **3** show that overall the structure is a good model for the measured data set.

Structure analysis and refinement. The structure was solved by direct methods (SHELXS-97);[68] refinement was done by full-matrix least squares on F^2 using the SHELXL-97 program suite;[68] empirical (multi-scan) absorption correction with SADABS.[69] All non-hydrogen positions were refined with anisotropic temperature factors. Hydrogen atoms were positioned geometrically and refined using a riding model (AFIX 43 for aromatic CH, AFIX 13 for aliphatic CH and AFIX 23 for CH_2)

Table 5 Crystal data for compounds **1**, **3** and **7–9**

	1	**3**	**7**	**8**	**9**
Empirical formula	$C_8H_{24}Br_2Cu_3N_4O_4$	$C_{32}H_{80}Br_4Cu_6N_8O_8$[e]	$C_{29}H_{77}Br_8Cu_6N_7O_8$	$C_{28}H_{74}Cl_8Cu_6N_6O_8$	$C_{16}H_{46}Cl_2Cu_2N_4O_{14}$
M/g mol^{-1}	590.75	1405.92	1672.50	1287.77	716.55
Crystal size/mm^3	$0.20 \times 0.20 \times <0.01$	$0.15 \times 0.15 \times <0.01$	$0.05 \times 0.01 \times 0.01$	$0.10 \times 0.01 \times 0.01$	$0.10 \times 0.08 \times 0.03$
Temperature/K	100(2)	118(2)	103(2)	103(2)	100(2)
θ range/° (completeness)	2.46–26.36 (98.90%)	3.11–25.00 (99.8)	1.87–18.85 (99.7)	1.05–22.21 (99.9)	1.25–23.49 (99.8)
h; k; l range	±10; −10, 11; ±14	±10; ±13; ±14	±9; ±11; −16, 18	±11, ±13, ±20	±18; ±18; ±6
Crystal system	Monoclinic	Triclinic	Monoclinic	Monoclinic	Orthorhombic
Space group	$P2_1/c$	$P1$	$P2_1$	$P2_1$	$P2_12_12$
a/Å	8.7424(2)	9.0782(18)	10.2700(17)	10.3649(3)	16.2260(3)
b/Å	8.9246(2)	11.603(2)	12.8186(16)	12.7064(3)	16.2256(3)
c/Å	11.6251(3)	12.489(3)	20.588(3)	19.3781(5)	5.6010(1)
α/°	90	102.76(3)	90	90	90
β/°	108.5920(10)	100.94(3)	93.281(8)	92.255(2)	90
γ/°	90	90.00(3)[f]	90	90	90
V/Å^3	859.68(4)	1258.4(4)	2706.0(7)	2550.13(12)	1474.61(5)
Z	2	1	2	2	2
D_{calc}/g cm^{-3}	2.282	1.855	2.053	1.677	1.614
μ (Mo Kα)/mm^{-1}	8.342	5.715	8.268	2.921	1.690
F(000)	578	706	1636	1316	748
Max./min. transmission	0.9212/0.2862	0.9451/0.4811	0.9219/0.6826	0.9714/0.7588	0.9510/0.8492
Reflections collected	10595	8784	9898	45441	30712
Independent reflect. (R_{int})	1737 (0.0402)	8784	4223 (0.0861)	6422 (0.1089)	2177 (0.0381)
Data/restraints/parameters	1737/0/97	8784/549/529	4223/429/538	6422/811/616	2177/296/198
Max./min. $\Delta\rho$/e Å^{-3}[a]	2.902/−0.967	3.798/−2.724	1.187/−0.639	0.572/−0.587	1.520/−0.679
$R1/wR2$ [$I > 2\sigma(I)$][b]	0.0366/0.0924	0.0994/0.2423	0.0649/0.1260	0.0493/0.0909	0.0539/0.1476
$R1/wR2$ (all data)[b]	0.0473/0.0991	0.1358/0.2730	0.1149/0.1502	0.0959/0.1092	0.0581/0.1523
Goodness-of-fit on F^2[c]	1.042	0.994	1.039	1.039	1.051
Flack parameter[d]	—	0.00(3)	0.04(4)	0.00(2)	0.00(1)

[a] Largest difference peak and hole. [b] $R_1 = [\sum(\|F_o|-|F_c\|)/\sum|F_o|]$; $wR_2 = [\sum[w(F_o^2 - F_c^2)^2]/\Sigma[w(F_o^2)^2]]^{1/2}$. [c] Goodness-of-fit $= [\sum[w(F_o^2 - F_c^2)^2]/(n-p)]^{1/2}$. [d] Absolute structure parameter.[74] [e] Two symmetry-independent formula units of $C_{16}H_{40}Br_2Cu_3N_4O_4$. [f] In compound **3** the protruding or interlocking ethyl groups shift the layers along the *a*-axis relative to the *b*-axis (*cf.* Fig. 4 and Fig. S11, ESI). Hence, one of the 90° angles present in compound **1** is 'lost', and only a triclinic space group becomes possible, despite the existence of pseudo-C_2 symmetry elements in the SBUs and within a layer. This leads to a triclinic space group with one remaining 90° angle.

with $U_{iso}(H) = 1.2\ U_{eq}(CH)$. For CH_3 AFIX 137 was used with $U_{iso}(H) = 1.5\ U_{eq}(CH)$. For compounds **7** and **8** the thermal parameters are high but no disorder was refined because of the already poor data/parameter ratio.

Compound **9** crystallizes in the orthorombic space group $P2_12_12$ (no. 18), which is a maximal non-isomorphic subgroup of tetragonal $P\bar{4}2_1m$ (no. 113). The data were also refined in the latter space group. With a = 16.2260(3) and b = 16.2256(3) the axes are not very different; within the esds they are the same and PLATON[67] suggests $P\bar{4}2_1m$ when the data are checked for missed symmetry. $P\bar{4}2_1m$ is a very rare space group with only 184 structures with this space group are published in the CSD.[70] In both space groups the perchlorate is severely disordered. The R-value is better in $P2_12_12$ (5.4%) than in $P\bar{4}2_1m$ (7.8%). Also, the thermal displacement parameters are larger in $P\bar{4}2_1m$. The data in $P2_12_12$ were refined with a twin law for swapped a- and b-axes with additional racemic twinning of both possibilities (0 1 0 –1 0 0 0 0 1 –4; BASF 0.11537 0.15813 0.38834).

Crystal data and details on the structure refinement are given in Table 5. Graphics were drawn with DIAMOND.[71]

Computational details

Spin-unrestricted DFT calculations were performed at the B3LYP level by means of the Gaussian09 code.[72] The structure of the trinuclear units were not optimized and the atomic positions were directly taken from X-ray cif files. Single-point calculations were performed for both the quartet, HS, with $\langle S^2 \rangle \approx 3.75$ and the broken symmetry, BS, with $\langle S^2 \rangle \approx 1.75$ states. For the case of compound **3** the calculations were performed in only one of the two trinuclear units. A triple-ξ all-electron Gaussian basis set was used for all elements.[73]

Acknowledgements

This work was supported by DFG grant Ja466/14-1.

References

1 L. Ma, C. Abney and W. Lin, *Chem. Soc. Rev.*, 2009, **38**, 1248–1256; C. Janiak and J. K. Vieth, *New J. Chem.*, 2010, **34**, 2366–2388; C. Janiak, *Dalton Trans.*, 2003, 2781–2804; C. Janiak, *Angew. Chem., Int. Ed. Engl.*, 1997, **36**, 1431–1434.

2 H.-J. Kim, J.-K. Kim and M. Lee, *Chem. Commun.*, 2010, **46**, 1458–1460; D. L. Reger, J. Horger, M. D. Smith and G. J. Long, *Chem. Commun.*, 2009, 6219–6221; C. Livage, N. Guillou, P. Rabu, P. Pattison, J. Marrot and G. Férey, *Chem. Commun.*, 2009, 4551–4553; L. Wang, J.-C. Chambron and E. Espinosa, *New J. Chem.*, 2009, **33**, 327–336; D.-K. Bučar, G. S. Papaefstathiou, T. D. Hamilton and L. R. MacGillivray, *New J. Chem.*, 2008, **32**, 797–799; L. Sbircea, N. D. Sharma, W. Clegg, R. W. Harrington, P. N. Horton, M. B. Hursthouse, D. C. Apperley, D. R. Boyd and S. L. James, *Chem. Commun.*, 2008, 5538–5540.

3 B. Gil-Hernández, J. K. Maclaren, H. A. Höppe, J. Pasan, J. Sanchiz and C. Janiak, *CrystEngComm*, 2012, **14**, 2635–2644; B. Gil-Hernández, H. A. Höppe, J. K. Vieth, J. Sanchiz and C. Janiak, *Chem. Commun.*, 2010, **46**, 8270–8272; Z. F. Chen, S. F. Zhang, H. S. Luo, B. F. Abrahams and H. Liang, *CrystEngComm*, 2007, **9**, 27–29; B.-Y. Lou, R.-H. Wang, D.-Q. Yuan, B.-L. Wu, F.-L. Jiang and M.-C. Hong, *Inorg. Chem. Commun.*, 2005, **8**, 971–974; J. Zhang, Y. Kang, R.-B. Zhang, Z.-J. Li, J.-K. Cheng and Y.-G. Yao, *CrystEngComm*, 2005, **7**, 177–178; V. Balamurugan and R. Mukherjee, *CrystEngComm*, 2005, **7**, 337–341; R. Peng, T. Wu and D. Li, *CrystEngComm*, 2005, **7**, 595–598; B. Lou, X. Huang and X. Lin, *Z. Anorg. Allg. Chem.*, 2007, **633**, 372–374.

4 J. Weng, M. Hong, Q. Shi, R. Cao and A. S. C. Chan, *Eur. J. Inorg. Chem.*, 2002, **2002**, 2553–2556.

5 Z.-X. Wang, M.-X. Li, M. Shao and H.-P. Xiao, *Inorg. Chem. Commun.*, 2009, **12**, 201–203.

6 J. S. Seo, D. Whang, H. Lee, S. I. Jun, J. Oh, Y. J. Jeon and K. Kim, *Nature*, 2000, **404**, 982–986.

7 C. Valente, E. Choi, M. E. Belowich, C. J. Doonan, Q. Li, T. B. Gasa, Y. Y. Botros, O. M. Yaghi and J. F. Stoddart, *Chem. Commun.*, 2010, **46**, 4911–4913.

8 O. Mamula and A. von Zelewsky, *Coord. Chem. Rev.*, 2003, **242**, 87–95; E. Barea, J. A. R. Navarro, J. M. Salas, M. Quirós, M. Willermann and B. Lippert, *Chem.–Eur. J.*, 2003, **9**, 4414–4421.

9 S. Hasegawa, S. Horike, R. Matsuda, S. Furukawa, K. Mochizuki, Y. Kinoshita and S. Kitagawa, *J. Am. Chem. Soc.*, 2007, **129**, 2607–2614.

10 B. F. Abrahams, M. Moylan, S. D. Orchard and R. Robson, *Angew. Chem., Int. Ed.*, 2003, **42**, 1848–1851.

11 R. Vaidhyanathan, D. Bradshaw, J.-N. Rebilly, J. P. Barrio, J. A. Gould, N. G. Berry and M. J. Rosseinsky, *Angew. Chem., Int. Ed.*, 2006, **45**, 6495–6499; E. V. Anokhina and A. J. Jacobson, *J. Am. Chem. Soc.*, 2004, **126**, 3044–3045; S.-P. Wu and C.-H. Lee, *CrystEngComm*, 2009, **11**, 219–222.

12 Z.-F. Chen, J. Zhang, R.-G. Xiong and X.-Z. You, *Inorg. Chem. Commun.*, 2000, **3**, 493–496; R.-G. Xiong, J.-L. Zuo, X.-Z. You, H.-K. Fun and S. S. S. Raj, *New J. Chem.*, 1999, **23**, 1051–1052; D. N. Dybtsev, A. L. Nuzhdin, H. Chun, K. P. Bryliakov, E. P. Talsi, V. P. Fedin and K. Kim, *Angew. Chem., Int. Ed.*, 2006, **45**, 916–920.

13 S. Thushari, J. A. K. Cha, H. H. Y. Sung, S. S. Y. Chui, A. L. F. Leung, Y.-F. Yen and I. D. Williams, *Chem. Commun.*, 2005, 5515–5517; A. S. F. Au-Yeung, H. H. Y. Sung, J. A. K. Cha, A. W. H. Siu, S. S. Y. Chui and I. D. Williams, *Inorg. Chem. Commun.*, 2006, **9**, 507–511.

14 P. Thuéry, *CrystEngComm*, 2007, **9**, 460–462.

15 Y. L. Bai, J. Tao, R. B. Huang and L. S. Zheng, *CrystEngComm*, 2008, **10**, 472–474; J.-Q. Liu, Y.-Y. Wang, P. Liu, W.-P. Wu, Y.-P. Wu, X.-R. Zeng, F. Zhong and Q.-Z. Shi, *Inorg. Chem. Commun.*, 2007, **10**, 343–347.

16 A. Beghidja, G. Rogez, P. Rabu, R. Welter and M. Drillon, *J. Mater. Chem.*, 2006, **16**, 2715–2728.

17 X.-Q. Liang, D.-P. Li, C.-H. Li, X.-H. Zhou, Y.-Z. Li, J.-L. Zuo and X.-Z. You, *Cryst. Growth Des.*, 2010, **10**, 2596–2605; J. Zhang, Y. G. Yao and X. Bu, *Chem. Mater.*, 2007, **19**, 5083–5089; J. Zhang, S. Chen, H. Valle, M. Wong, C. Austria, M. Cruz and X. Bu, *J. Am. Chem. Soc.*, 2007, **129**, 14168–14169; J. A. Rood, W. C. Boggess, B. C. Noll and K. W. Henderson, *J. Am. Chem. Soc.*, 2007, **129**, 13675–13682; J. Zhang, R. Liu, P. Feng and X. Bu, *Angew. Chem., Int. Ed.*, 2007, **46**, 8388–8391; J. Zhang and X. Bu, *Angew. Chem., Int. Ed.*, 2007, **46**, 6115–6118; D. N. Dybtsev, M. P. Yutkin, E. V. Peresypkina, A. V. Virovets, C. Serre, G. Férey and V. P. Fedin, *Inorg. Chem.*, 2007, **46**, 6843–6845; P. Guo, *Dalton Trans.*, 2011, **40**, 1716–1721; J. Zhang and X. Bu, *Chem. Commun.*, 2009, 206–208.

18 B. Wisser, A.-C. Chamayou, R. Miller, W. Scherer and C. Janiak, *CrystEngComm*, 2008, **10**, 461–464; Z. Chen, X. Liu, C. Zhang, Z. Zhang and F. Liang, *Dalton Trans.*, 2011, **40**, 1911–1918.

19 D. Mekhatria, S. v. Rigolet, C. Janiak, A. l. Simon-Masseron, M. A. Hasnaoui and A. Bengueddach, *Cryst. Growth Des.*, 2011, **11**, 396–404; B. Wisser, Y. Lu and C. Janiak, *Z. Anorg. Allg. Chem.*, 2007, **633**, 1189–1192; G. Vujevic and C. Janiak, *Z. Anorg. Allg. Chem.*, 2003, **629**, 2585–2590; L.-F. Ma, L.-Y. Wang, J.-G. Wang, Y.-F. Wang and X. Feng, *Z. Anorg. Allg. Chem.*, 2006, **632**, 487–490.

20 M. Enamullah, A. Sharmin, M. Hasegawa, T. Hoshi, A.-C. Chamayou and C. Janiak, *Eur. J. Inorg. Chem.*, 2006, 2146–2154.

21 B. Paul, C. Näther, K. M. Fromm and C. Janiak, *CrystEngComm*, 2005, **7**, 309–319.

22 A.-C. Chamayou, S. Lüdeke, V. Brecht, T. B. Freedman, L. A. Nafie and C. Janiak, *Inorg. Chem.*, 2011, **50**, 11363–11374; C. Janiak, A.-C. Chamayou, A. K. M. Royhan Uddin, M. Uddin, K. S. Hagen and M. Enamullah, *Dalton Trans.*, 2009, 3698–3709; M. Enamullah, A. Uddin, A. C. Chamayou and C. Janiak, *Z. Naturforsch., B*, 2007, **62b**, 807–817.

23 M. J. Plater, T. Gelbrich, M. B. Hursthouse and B. M. D. Silva, *CrystEngComm*, 2006, **8**, 895–903; D. G. Billing and A. Lemmerer, *CrystEngComm*, 2006, **8**, 686–695; S. George, S. Lipstman, S. Muniappan and I. Goldberg, *CrystEngComm*, 2006, **8**, 417–424; R. Peng, T. Wu and D. Li, *CrystEngComm*, 2005, **7**, 595–598; B. Wisser and C. Janiak, *Z. Anorg. Allg. Chem.*, 2007, **633**, 1796–1800.
24 A. N. Parvulescu, G. Marin, K. Suwinska, V. C. Kravtsov, M. Andruh, V. Parvulescu and V. I. Parvulescu, *J. Mater. Chem.*, 2005, **15**, 4234–4240; V. Tudor, G. Marin, V. Kravtsov, Y. A. Simonov, J. Lipkowski, M. Brezeanu and M. Andruh, *Inorg. Chim. Acta*, 2003, **353**, 35–42; C. Paraschiv, M. Andruh, S. Ferlay, M. W. Hosseini, N. Kyritsakas, J. M. Planeix and N. Stanica, *Dalton Trans.*, 2005, 1195–1202; H. W. Roesky and M. Andruh, *Coord. Chem. Rev.*, 2003, **236**, 91–119; H. Muhonen, *Acta Chem. Scand., Ser. A*, 1980, **34**, 79–83; H. Muhonen, W. E. Hatfield and J. H. Helms, *Inorg. Chem.*, 1986, **25**, 800–805; R. Mergehenn, W. Haase and R. Allmann, *ActaCrystallogr., Sect. B: Struct. Crystallogr. Cryst. Chem.*, 1975, **31**, 1847–1853; L. Merz and W. Haase, *J. Chem. Soc., Dalton Trans.*, 1978, 1594–1598; L. Schwabe and W. Haase, *Acta Crystallogr., Sect. C: Cryst. Struct. Commun.*, 1986, **42**, 667–669; R. Mergehenn, L. Merz and W. Haase, *J. Chem. Soc., Dalton Trans.*, 1980, 1703–1709; D. Masi, C. Mealli, M. Sabat, A. Sabatini, A. Vacca and F. Zanobini, *Helv. Chim. Acta*, 1984, **67**, 1818–1826; U. Turpeinen, R. Hämäläinen and J. Reedijk, *Inorg. Chim. Acta*, 1988, **154**, 201–207; S. Putzien, S. Wirth, J. Nicolas Roedel and I.-P. Lorenz, *Polyhedron*, 2011, **30**, 1747–1751; R. Mergehenn and W. Haase, *Acta Crystallogr., Sect. B: Struct. Crystallogr. Cryst. Chem.*, 1977, **33**, 1877–1882; R. Mergehenn and W. Haase, *Acta Crystallogr., Sect. B: Struct. Crystallogr. Cryst. Chem.*, 1977, **33**, 2734–2739; J. Saßmannshausen, H. G. von Schnering and L. Walz, *Z. Kristallogr.*, 1997, **212**, 656–661; A. Pajunen and K. Nieminen, *Finn. Chem. Lett*, 1975, 67–70; K. Nieminen, *Acta Chem. Scand., Ser. A*, 1977, **31A**, 693–699; K. Nieminen and A. Pajunen, *Acta Chem. Scand., Ser. A*, 1978, **32A**, 493–499; A. Pajunen, *Acta Crystallogr., Sect. B: Struct. Crystallogr. Cryst. Chem.*, 1979, **35**, 1691–1693; K. Nieminen, *Acta Chem. Scand., Ser. A*, 1979, **33A**, 375–381; Z. X. Wang, X. L. Li, B. L. Liu, H. Tokoro, P. Zhang, Y. Song, S. I. Ohkoshi, K. Hashimoto and X. Z. You, *Dalton Trans.*, 2008, 2103–2106; U. Turpeinen, R. Hamalanen and I. Mutikainen, *Acta Crystallogr., Sect. C: Cryst. Struct. Commun.*, 1999, **55**, 50–52; U. Turpeinen, O. Orama, I. Mutikainen and R. Hämäläinen, *Z. Kristallogr.*, 1996, **211**, 867–869; U. Turpeinen, M. Klinga, I. Mutikainen and R. Hämäläinen, *Z. Kristallogr. - New Cryst. Struct.*, 2000, **215**, 418–420; U. Turpeinen, R. Hamalainen, I. Mutikainen and O. Orama, *Acta Crystallogr., Sect. C: Cryst. Struct. Commun.*, 1996, **52**, 568–570; M. Shahid, A. A. Tahir, M. Hamid, M. Mazhar, M. Zeller, K. C. Molloy and A. D. Hunter, *Eur. J. Inorg. Chem.*, 2009, **2009**, 1043–1050; M. Shahid, M. Mazhar, M. Hamid, P. O'Brien, M. A. Malik and M. Helliwell, *Appl. Organomet. Chem.*, 2010, **24**, 714–720.
25 G. Marin, M. Andruh, A. M. Madalan, A. J. Blake, C. Wilson, N. R. Champness and M. Schröder, *Cryst. Growth Des.*, 2008, **8**, 964–975.
26 G. Marin, V. Tudor, V. C. Kravtsov, M. Schmidtmann, Y. A. Simonov, A. Muller and M. Andruh, *Cryst. Growth Des.*, 2004, **5**, 279–282.
27 G. Marin, V. Kravtsov, Y. A. Simonov, V. Tudor, J. Lipkowski and M. Andruh, *J. Mol. Struct.*, 2006, **796**, 123–128.
28 S. Kimmo, *Inorg. Chim. Acta*, 1987, **128**, 61–68.
29 S. R. Breeze, S. Wang and L. Chen, *J. Chem. Soc., Dalton Trans.*, 1996, 1341–1349.
30 A. Pajunen and K. Smolander, *Finn. Chem. Lett.*, 1974, **1974**, 99; Y. Song, D.-R. Zhu, K.-L. Zhang, Y. Xu, C.-Y. Duan and X.-Z. You, *Polyhedron*, 2000, **19**, 1461–1464; E. A. Vinogradova, O. Y. Vassilyeva, V. N. Kokozay and B. W. Skeleton, *Z. Naturforsch., B*, 2002, **57b**, 319.
31 L. Dahlenburg, H. Treffert, C. Farr, F. W. Heinemann and A. Zahl, *Eur. J. Inorg. Chem.*, 2007, **2007**, 1738–1751.
32 G. Nieuwpoort, G. C. Verschoor and J. Reedijk, *J. Chem. Soc., Dalton Trans.*, 1983, 531–538; H. Fric, M. Puchberger and U. Schubert, *Eur. J. Inorg. Chem.*, 2008, 1452–1461.
33 F. Accadbled, B. Tinant, E. Henon, D. Carrez, A. Croisy and S. Bouquillon, *Dalton Trans.*, 2010, **39**, 8982–8993.
34 T. Koura and Y. Ohashi, *Tetrahedron*, 2000, **56**, 6769–6779.
35 K. Meelich, M. Galanski, V. B. Arion and B. K. Keppler, *Eur. J. Inorg. Chem.*, 2006, 2476–2483; B. M. Louie, S. J. Rettig, A. Storr and J. Trotter, *Can. J. Chem.*, 1985, **63**, 2261–2272; M. Galanski, C. Baumgartner, V. Arion and B. K. Keppler, *Eur. J. Inorg. Chem.*, 2003, 2619–2625.
36 Y. Ohgo, Y. Arai, M. Hagiwara, S. Takeuchi, H. Kogo, A. Sekine, H. Uekusa and Y. Ohashi, *Chem. Lett.*, 1994, **23**, 715–718.
37 A. M. Manotti Lanfredi, A. Tiripicchio and M. Tiripicchio Camellini, *Acta Crystallogr., Sect. B: Struct. Crystallogr. Cryst. Chem.*, 1979, **35**, 349–353; J. G. Wardeska, A. Clearfield and J. M. Troup, *Inorg. Chem.*, 1979, **18**, 1641–1648; A. Clearfield, P. Rudolf and J. G. Wardeska, *Inorg. Chem.*, 1983, **22**, 2713–2716; R. E. Benson, A. Clearfield, L. M. Daniels and J. G. Wardeska, *Acta Crystallogr., Sect. E: Struct. Rep. Online*, 2006, **62**, m696–m698.
38 Y. Ohashi, Y. Sasada, Y. Tashiro, Y. Ohgo, S. Takeuchi and J. Yoshimur, *Bull. Chem. Soc. Jpn.*, 1973, **46**, 2589–2590; M. Hennig, K. Päntener and M. Scalone, *Tetrahedron: Asymmetry*, 2000, **11**, 1849–1858.
39 H. Amano, A. Sekine, Y. Ohashi, M. Hagiwara, J. Sato, Y. Arai and Y. Ohgo, *Bull. Chem. Soc. Jpn.*, 1996, **69**, 3107–3114.
40 J. F. Malone, M. Miskelly and M. Parvez, *Proc. R. Ir. Acad., Sect. B*, 1977, **77**, 499–506.
41 T. Dorn, C. Janiak and K. Abu-Shandi, *CrystEngComm*, 2005, **7**, 633–641.
42 B. Paul, C. Näther, B. Walfort, K. M. Fromm, B. Zimmermann, H. Lang and C. Janiak, *CrystEngComm*, 2004, **6**, 293–297.
43 T. Dorn, A.-C. Chamayou and C. Janiak, *New J. Chem.*, 2006, **30**, 156–167.
44 τ = (difference between the two largest angles)/60 for five-coordinated metal centers allows for the distinction between trigonal-bipyramidal (ideally $\tau = 1$) and square-pyramidal (ideally $\tau = 0$): A. W. Addison, T. N. Rao, J. Reedijk, J. van Rijnn and G. C. Verschoor, *J. Chem. Soc., Dalton Trans.*, 1984, 1349–1356.
45 A.-C. Chamayou, M. A. Neelakantan, S. Thalamuthu and C. Janiak, *Inorg. Chim. Acta*, 2011, **365**, 447–450; B. M. Drašković, G. A. Bogdanović, M. A. Neelakantan, A.-C. Chamayou, S. Thalamuthu, Y. S. Avadhut, J. Schmedt auf der Günne, S. Banerjee and C. Janiak, *Cryst. Growth Des.*, 2010, **10**, 1665–1676; H. A. Habib, B. Gil-Hernández, K. Abu-Shandi, J. Sanchiz and C. Janiak, *Polyhedron*, 2010, **29**, 2537–2545; F. Zhuge, B. Wu, J. Liang, J. Yang, Y. Liu, C. Jia, C. Janiak, N. Tang and X.-J. Yang, *Inorg. Chem.*, 2009, **48**, 10249–10256; B. Wu, J. Liang, J. Yang, C. Jia, X.-J. Yang, H. Zhang, N. Tang and C. Janiak, *Chem. Commun.*, 2008, 1762–1764; B. Wu, X. Huang, Y. Xia, X.-J. Yang and C. Janiak, *CrystEngComm*, 2007, **9**, 676–685; M. D. Ward, *Chem. Commun.*, 2005, 5838–5842.
46 P. Raghavaiah, S. Supriya and S. K. Das, *CrystEngComm*, 2005, **7**, 167–170.
47 R. A. Vaia and W. Liu, *J. Polym. Sci., Part B: Polym. Phys.*, 2002, **40**, 1590–1600.
48 S. Myllyviita, R. Sillanpaa, J. J. A. Kolnaar and J. Reedijk, *J. Chem. Soc., Dalton Trans.*, 1995, 2209–2213.
49 O. Kahn, *Molecular Magnetism*, VCH, New York, 1993.
50 S. Ferrer, F. Lloret, I. Bertomeu, G. Alzuet, J. Borrás, S. García-Granada, M. Liu-González and J. G. Haasnoot, *Inorg. Chem.*, 2002, **41**, 5821–5830.
51 Y. Ma, Y. Q. Wen, J. Y. Zhang, E. Q. Gao and C. M. Liu, *Dalton Trans.*, 2010, **39**, 1846–1854; J. Garcia-Gimenez, G. Alzueta, M. Gonzalez-Alvarez, M. Liu-Gonzalez, A. Castineiras and J. Borras, *J. Inorg. Biochem.*, 2009, **103**, 243–255.
52 Z. Boulsourani, V. Tangoulis, C. P. Raptopoulou, V. Psycharis and C. Dendrinou-Samara, *Dalton Trans.*, 2011, **40**, 7946–7956.
53 A. M. Kirillov, Y. Y. Karabach, M. Haukka, M. F. C. Guedes da Silva, J. Sanchiz, M. N. Kopylovich and A. J. L. Pombeiro, *Inorg. Chem.*, 2008, **47**, 162–175.
54 V. H. Crawford, H. W. Richardson, J. R. Wasson, D. J. Hodgson and W. E. Hatfield, *Inorg. Chem.*, 1976, **15**, 2107–2110.
55 E. Ruiz, P. Alemany, S. Alvarez and J. Cano, *J. Am. Chem. Soc.*, 1997, **119**, 1297–1303; E. Ruiz, P. Alemany, S. Alvarez and J. Cano, *Inorg. Chem.*, 1997, **36**, 3683; R. P. Doyle, M. Julve, F. Lloret, M. Nieuwenhuyzen and P. E. Kruger, *Dalton Trans.*, 2006, 2081.
56 M. Du, X.-J. Zhao, J.-H. Guo, X.-H. Bu and J. Ribas, *Eur. J. Inorg. Chem.*, 2005, 294–394.

57 L. Merz and W. Haase, *J. Chem. Soc., Dalton Trans.*, 1980, 875–879; M. Handa, N. Koga and S. Kida, *Bull. Chem. Soc. Jpn.*, 1988, **61**, 3853–3857.
58 Y. Song, P. Gamez, O. Roubeau, I. Mutikainen, U. Turpeinen and J. Reedijk, *Inorg. Chim. Acta*, 2005, **358**, 109–115.
59 Y. F. Song, G. A. van Albada, M. Quesada, I. Mutikainen, U. Turpeinen and J. Reedijk, *Inorg. Chem. Commun.*, 2005, **8**, 975–978.
60 S. H. Yan, X. J. Zheng, L. C. Li, D. Q. Yuan and L. P. Jin, *Dalton Trans.*, 2011, **40**, 1758–1767.
61 E. Ruiz, A. Rodriguez-Fortea, J. Cano, S. Alvarez and P. Alemany, *J. Comput. Chem.*, 2003, **24**, 982–989; T. C. Stamatatos, G. S. Papaefstathiou, R. MacGillivray, A. Escuer, R. Vicente, E. Ruiz and S. P. Perlepes, *Inorg. Chem.*, 2007, **46**, 8843–8850.
62 E. Ruiz, J. Cano, S. Alvarez and P. Alemany, *J. Comput. Chem.*, 1999, **20**, 1391–1400.
63 *WinXPOW, Version 1.10*, STOE & Cie GmbH, Darmstadt, Germany, 2002.
64 *APEX2, data collection program for the CCD area-detector system, Version 2.1-0*, Bruker Analytical X-ray Systems, Madison, WI, 2006.
65 *SAINT, data reduction and frame integration program for the CCD area-detector system*, Bruker Analytical X-ray Systems, Madison, WI, 2006.
66 *CrystalClearSM, 1.4.0*. Rigaku Coorporation, Tokyo, Japan, 2007.
67 A. L. Spek, *J. Appl. Crystallogr.*, 2003, **36**, 7–13; *PLATON–A Multipurpose Crystallographic Tool*, Utrecht University, Utrecht, The Netherlands, 2008; Windows implementation: L. J. Farrugia, University of Glasgow, Scotland, Version 40608, 2008.
68 G. M. Sheldrick, *Acta Crystallogr., Sect. A: Found. Crystallogr.*, 2008, **A64**, 112–122.
69 G. M. Sheldrick, *Program SADABS*, University of Göttingen, Göttingen, Germany, 1996.
70 Cambridge Structural Database, CSD Space Group Statisctic – Space Group Number Ordering; 1 January 2012; http://www.ccdc.cam.ac.uk/products/csd/statistics/stats_sgnumorder_Jan2012.pdf.
71 K. Brandenburg, *Diamond (Version 3.2c), crystal and molecular structure visualization, Crystal Impact*, K. Brandenburg & H. Putz Gbr, Bonn, Germany, 2009.
72 M. J. Frisch, *in Gaussian 09, revision A1*, Gaussian. Inc, Wallinford, 2009.
73 A. Scheafer, C. Huber and R. Ahlrichs, *J. Chem. Phys.*, 1994, **100**, 5829–5835.
74 H. D. Flack, M. Sadki, A. L. Thompson and D. J. Watkin, *Acta Crystallogr., Sect. A: Found. Crystallogr.*, 2011, **67**, 21–34; H. D. Flack and G. Bernardinelli, *Chirality*, 2008, **20**, 681–690; H. D. Flack and G. Bernardinelli, *Acta Crystallogr., Sect. A: Found. Crystallogr.*, 1999, **55**, 908–915; H. D Flack, *Acta Crystallogr., Sect. A: Found. Crystallogr.*, 1983, **39**, 876–881.